

## LUMPED PARAMETER MODELS FOR THE INTERPRETATION OF ENVIRONMENTAL TRACER DATA

P. MALOSZEWSKI  
GSF-Institute for Hydrology  
Oberschleissheim,  
Germany

A. ZUBER  
Institute of Nuclear Physics,  
Cracow, Poland

### Abstract

Principles of the lumped-parameter approach to the interpretation of environmental tracer data are given. The following models are considered: the piston flow model (PFM), exponential flow model (EM), linear model (LM), combined piston flow and exponential flow model (EPM), combined linear flow and piston flow model (LPM), and dispersion model (DM). The applicability of these models for the interpretation of different tracer data is discussed for a steady state flow approximation. Case studies are given to exemplify the applicability of the lumped-parameter approach. Description of a user-friendly computer program is given.

### 1. Introduction

#### 1.1. Scope and history of the lumped-parameter approach

This manual deals with the lumped-parameter approach to the interpretation of environmental tracer data in aquifers. In a *lumped-parameter model* or a *black-box model*, the system is treated as a whole and the flow pattern is assumed to be constant. Lumped-parameter models are the simplest and best applicable to systems containing young water with modern tracers of variable input concentrations, e.g., tritium, Kr-85 and freons, or seasonably variable  $^{18}\text{O}$  and  $^2\text{H}$ . The concentration records at the recharge area must be known or estimated, and for measured concentrations at outflows (e.g. springs and abstraction wells), the global parameters of the investigated system are found by a trial-and-error procedure. Several simple models commonly applied to large systems with a constant tracer input (e.g. the piston flow model usually applied to the interpretation of radiocarbon data) also belong to the category of the lumped-parameter approach and are derivable from the general formula.

The manual contains basic definitions related to the tracer method, outline of the lumped-parameter approach, discussion of different types of flow models represented by system response functions, definitions and discussion of the parameters of the response functions, and selected case studies. The case studies are given to demonstrate the following problems: difficulties in obtaining a unique calibration, relation of tracer ages to flow and rock parameters in granular and fissured systems, application of different tracers to some complex systems. Appendix A contains examples of response functions for different injection-detection modes. Appendix B contains an example of differences between the water age, the conservative

tracer age, and the radioisotope age for a fissured aquifer. Appendix C contains user's guide to the FLOW - a computer program for the interpretation of environmental tracer data in aquifers by the lumped-parameter approach, which is supplied on a diskette. [\*]

The interpretation of tracer data by the lumped-parameter approach is particularly well developed in chemical engineering. The earliest quantitative interpretations of environmental tracer data for groundwater systems were based on the simplest models, i.e., either the piston flow model or the exponential model (mathematically equivalent to the well-mixed cell model), which are characterized by a single parameter [1]. A little more sophisticated two-parameter model, represented by binomial distribution was introduced in late 1960s [2]. Other two-parameter models, i.e., the dispersion model characterized by a uni-dimensional solution to the dispersion equation, and the piston flow model combined with the exponential model, were shown to yield better fits to the experimental results [3]. All these models have appeared to be useful for solving a number of practical problems, as it will be discussed in sections devoted to case studies. Recent progress in numerical methods and multi-level samplers focused the attention of modelers on two- and three-dimensional solutions to the dispersion equation. However, the lumped-parameter approach still remains to be a useful tool for solving a number of practical problems. Unfortunately, this approach is often ignored by some investigators. For instance, in a recent review [4] a general description of the lumped-parameter approach was completely omitted, though the piston flow and well-mixed cell models were given. The knowledge of the lumped-parameter approach and the transport of tracer in the simplest flow system is essential for a proper understanding of the tracer method and possible differences between flow and tracer ages. Therefore, even those who are not interested in the lumped-parameter approach are advised to get acquainted with the following text and particularly with the definitions given below, especially as some of these definitions are also directly or indirectly applicable to other approaches.

## 1.2. Useful definitions

In this manual we shall follow definitions taken from several recent publications [5, 6, 7, 8, 9] with slight modifications. However, it must be remembered that these definitions are not generally accepted and a number of authors apply different definitions, particularly in respect to such terms as model verification and model validation. Therefore, caution is needed, and, in the case of possible misunderstandings, the definitions applied should be either given or referred to an easily available paper. As far as verification and validation are concerned the reader is also referred to authors who are very critical about these terms used in their common meaning and who are of a opinion that they should be rejected as being highly misleading [10, 11].

The *tracer method* is a technique for obtaining information about a system or some part of a system by observing the behaviour of a specified substance, the tracer, that has been added to the system. Environmental tracers are added (injected) to the system by natural processes, whereas their production is either natural or results from the global activity of man.

---

[\*] User Guide and diskette are available free of charge from Isotope Hydrology Section, IAEA, Vienna, upon request.

An *ideal tracer* is a substance that behaves in the system exactly as the traced material as far as the sought parameters are concerned, and which has one property that distinguishes it from the traced material. This definition means that for an ideal tracer there should be neither sources nor sinks in the system other than those adherent to the sought parameters. In practice we shall treat as a good tracer even a substance which has other sources or sinks if they can be properly accounted for, or if their influence is negligible within the required accuracy.

A *conceptual model* is a qualitative description of a system and its representation (e.g. geometry, parameters, initial and boundary conditions) relevant to the intended use of the model.

A *mathematical model* is a mathematical representation of a conceptual model for a physical, chemical, and/or biological system by expressions designed to aid in understanding and/or predicting the behaviour of the system under specified conditions.

*Verification of a mathematical model*, or its computer code, is obtained when it is shown that the model behaves as intended, i.e. that it is a proper mathematical representation of the conceptual model and that the equations are correctly encoded and solved. A model should be verified prior to calibration.

*Model calibration* is a process in which the mathematical model assumptions and parameters are varied to fit the model to observations. Usually, calibration is carried out by a trial-and-error procedure. The calibration process can be quantitatively described by the goodness of fit.

Model calibration is a process in which the inverse problem is solved, i.e. from known input-output relations the values of parameters are determined by fitting the model results to experimental data. The direct problem is solved if for known or assumed parameters the output results are calculated (model prediction). Testing of hypotheses is performed by comparison of model predictions with experimental data.

*Validation* is a process of obtaining assurance that a model is a correct representation of the process or system for which it is intended. Ideally, validation is obtained if the predictions derived from a calibrated model agree with new observations, preferably for other conditions than those used for calibration. Contrary to calibration, the validation process is a qualitative one based on the modeller's judgment.

The term "a correct representation" may perhaps be misleading and too much promising. Therefore, a somewhat changed definition can be proposed: *Validation* is a process of obtaining assurance that a model satisfies the modeller's needs for the process or system for which it is intended, within an assumed or requested accuracy [9]. A model which was validated for some purposes and at a given stage of investigations, may appear invalidated by new data and further studies. However, this neither means that the validation process should not be attempted, nor that the model was useless.

*Partial validation* can be defined as validation performed with respect to some properties of a model [7, 8]. For instance, models represented by solutions to the transport equation yield proper solute velocities (i.e. can be validated in that respect - a partial validation), but usually do not yield proper dispersivities for predictions at larger scales.

In the case of the tracer method the validation is often performed by comparison of the values of parameters obtained from the models with those obtainable independently (e.g. flow velocity obtained from a model fitted to tracer data is shown to agree with that calculated from the hydraulic gradient and conductivity known from conventional observations [7, 8, 12, 13]. When results yielded by a model agree with results obtained independently, a number of authors state that the model is *confirmed*, e.g. [11], which is equivalent to the definition of validation applied within this manual.

The *direct problem* consists in finding the output concentration curve(s) for known or assumed input concentration, and for known or assumed

model type and its parameter(s). Solutions to the direct problem are useful for estimating the potential abilities of the method, for planning the frequency of sampling, and sometimes for preliminary interpretation of data, as explained below.

The *inverse problem* consists in searching for the model of a given system for which the input and output concentrations are known. Of course, for this purpose the graphs representing the solutions to the direct problem can be very helpful. In such a case the graph which can be identified with the experimental data will represent the solution to the inverse problem. A more proper way is realized by searching for the best fit model (calibration). Of course, a good fit is a necessary condition but not a sufficient one to consider the model to be validated (confirmed). The fitting procedure has to be used together with the geological knowledge, logic and intuition of the modeller [14]. This means that all the available information should be used in selecting a proper type of the model prior to the fitting. If the selection is not possible prior to the fitting, and if more than one model give equally good fit but with different values of parameters, the selection has to be performed after the fitting, as a part of the validation process. It is a common sin of modellers to be satisfied with the fit obtained without checking if other equally good fits are not available.

In dispersive dynamic systems, as aquifers, it is necessary to distinguish between different ways in which solute (tracer) concentration can be measured. The *resident concentration* ( $C_R$ ) expresses the mass of solute ( $\Delta m$ ) per unit volume of fluid ( $\Delta V$ ) contained in a given element of the system at a given instant,  $t$ :

$$C_R(t) = \Delta m(t)/\Delta V \quad (1)$$

The *flux concentration* ( $C_F$ ) expresses the ratio of the solute flux ( $\Delta m/\Delta t$ ) to the volumetric fluid flow ( $Q = \Delta V/\Delta t$ ) passing through a given cross-section:

$$C_F = \frac{\Delta m(t)/\Delta t}{\Delta V/\Delta t} = \frac{\Delta m(t)}{Q\Delta t} \quad (2)$$

The resident concentration can be regarded as the mean concentration obtained by weighting over a given cross-section of the system, whereas the flux concentration is the mean concentration obtained by weighting by the volumetric flow rates of flow lines through a given cross-section of the system. The differences between two types of concentration were shown either theoretically or experimentally by a number of authors [15, 16, 17, 18]. However, numerical differences between both types of concentration are of importance only for laminar flow in capillaries and for highly dispersive systems [18, 19] (see Appendix A).

The *turnover time* or *age of water leaving the system* ( $t_w$ ) is defined as:

$$t_w = V_m/Q \quad (3a)$$

where  $V_m$  is the volume of mobile water in the system. For systems which can be approximated by unidimensional flow, Eq. 3 reads:

$$t_w = V_m/Q = \frac{S_n x}{S_n v_w} = \frac{x}{v_w} \quad (3b)$$

where  $x$  is the length of the system measured along the streamlines,  $v_w$  is the mean velocity of water,  $n_e$  is the space fraction occupied by the mobile water (effective porosity), and  $S$  is the cross-section area normal to flow. According to Eq. 3b, the *mean water velocity* is defined as:

$$v_w = Q/(n_e S) = v_f/n_e \quad (4)$$

where  $v_f$  is *Darcy's velocity* defined as  $Q/S$ .

## 2. Immobile systems

Discussion of immobile systems is beyond the scope of this manual, but for the consistency of the age definitions they are briefly discussed below. For old groundwaters, a distinction should be made between mobile and immobile systems, especially in respect to the definition of age. A radioisotope tracer, which has no other source and sink than the radioactive decay, represents the age of water in an immobile system, if the system is separated from recharge and the mass transfer with adjacent systems by molecular diffusion is negligible. Then the *radioisotope age* ( $t_a$ ), understood as the time span since the separation event, is defined by the well known formula of the radioactive decay, and it should be the same in the whole system:

$$C/C(0) = \exp(-\lambda t_a) \quad (5)$$

where  $C$  and  $C(0)$  are the actual and initial radioisotope concentrations, and  $\lambda$  is the radioactive decay constant.

Unfortunately, ideal radioisotope tracers are not available for dating of old immobile water systems. Therefore, we shall mention that the accumulation of some tracers is a more convenient tool, if the accumulation rate can be estimated from the *in situ* production and the crust or mantle flux as it is in the case of  $^4\text{He}$  and  $^{40}\text{Ar}$  dating for both mobile and immobile systems. Similarly, the dependence of  $^2\text{H}$  and  $^{18}\text{O}$  contents in water molecules on the climatic conditions of recharge during different geological periods as well as noble gas concentrations expressed in terms of the temperature at the recharge area (noble gas temperatures) may also serve for reliable tracing of immobile groundwater systems in terms of ages.

## 3. Basic principles for constant flow systems

The *exit age-distribution function*, or the *transit time distribution*,  $E(t)$ , describes the exit time distribution of incompressible fluid elements of the system (water) which entered the system at a given  $t = 0$ . This function is normalized in such a way that:

$$\int_0^{\infty} E(t) dt = 1 \quad (6)$$

According to the definition of the  $E(t)$  function, the mean age of water leaving the system is:

$$t_w = \int_0^{\infty} tE(t) dt \quad (7)$$

The mean transit time of a tracer ( $t_t$ ) or the mean age of tracer is defined as:

$$t_t = \int_0^{\infty} t C_I(t) dt / \int_0^{\infty} C_I(t) dt \quad (8)$$

where  $C_I(t)$  is the tracer concentration observed at the measuring point as the result of an instantaneous injection at the injection point at  $t = 0$ . Equation 8 defines the age of any tracer injected and measured in any mode. In order to avoid possible misunderstandings, in all further considerations,  $t_t$  denotes the mean age of a conservative tracer. Unfortunately, it is a common mistake to identify Eq. 7 with Eq. 8 for conservative tracers (or for radioisotope tracers corrected for the decay) whereas the mean age of a conservative tracer leaving the system is equal to the mean age of water only if the tracer is injected and measured in the flux mode and if no stagnant water zones exist in the system. Consequently, because the tracer age may differ from the water age, it is convenient to define a function describing the distribution of a conservative tracer. This function, called the *weighting function*, or the *system response function*,  $g(t)$ , describes the exit age-distribution of tracer particles which entered the system of a constant flow rate at a given  $t = 0$ :

$$g(t) = C_I(t) / \int_0^{\infty} C_I(t) dt = C_I(t) Q / M \quad (9)$$

because the whole injected mass or activity ( $M$ ) of the tracer has to appear at the outlet, i.e.:

$$M = Q \int_0^{\infty} C_I(t) dt \quad (10)$$

As mentioned, the  $g(t)$  function is equal to the  $E(t)$  function, and, consequently, the mean age of tracer is equal to the turnover time of water, if a conservative tracer (or a decaying tracer corrected for the decay) is injected and measured in the flux mode, and if there are no stagnant zones in the system. Systems with stagnant zones are discussed in Sect. 9. In the lumped-parameter approach it is usually assumed that the concentrations are observed in water entering and leaving the system, which means that flux concentrations are applicable. Therefore, in all further considerations the  $C$  symbol stays for flux concentrations, and the mean transit time of tracer is equal to the mean transit time of water unless stated otherwise.

Equation 8 is of importance in artificial tracing, and, together with Eq. 9, serves for theoretical findings of the response functions in environmental tracing. For a steady flow through a groundwater system, the output concentration,  $C(t)$ , can be related to the input concentration ( $C_{in}$ ) of any tracer by the well known convolution integral:

$$C(t) = \int_0^{\infty} C_{in}(t-t') g(t') \exp(-\lambda t') dt' \quad (11a)$$

where  $t'$  is the transit time, or

$$C(t) = \int_{-\infty}^0 C_{in}(t') g(t-t') \exp[-\lambda(t-t')] dt' \quad (11b)$$

where  $t'$  is time of entry, and  $t - t'$  is the transit time.

The type of the model (e.g. the piston flow model, or dispersion model) is defined by the  $g(t')$  function chosen by the modeller whereas the model parameters are to be found by calibration (fitting of concentrations calculated from Eq. 11 to experimental data, for known or estimated input concentration records).

#### 4. Models and their parameters

##### 4.1. General

The lumped-parameter approach is usually limited to one- or two-parameter models. However, the type of the model and its parameters define the exit-age distribution function (the weighting function) which gives the spectrum of the transit times. Therefore, if the modeller gives just the type of the model and the mean age, the user of the data can be highly misled. Consider for instance an exponential model and the mean age of 50 years. The user who has no good understanding of the models may start to look for a relatively distant recharge area, and may think that there is no danger of a fast contamination. However, the exponential model (see Sects 4.3 and 9.1) means that the flow lines with extremely short (theoretically equal to zero) transit times exist. Therefore, the best practice is to report both the parameters obtained and the weighting function calculated for these parameters. Another possible misunderstanding is also related to the mean age. For instance, the lack of tritium means that no water recharged in the hydrogen-bomb era is present (i.e., after 1952). However, for highly dispersive systems (e.g. those described by the exponential model or the dispersive model with a large value of the dispersion parameter), the presence of tritium does not mean that an age of 100 years, or more, is not possible.

Sometimes either it is necessary to assume the presence of two water components (e.g., in river bank filtration studies), or it is impossible to obtain a good fit (calibration) without such an assumption. The additional parameter is denoted as  $\beta$ , and defined as the fraction of total water flow with a constant tracer concentration,  $C_{\beta}$ .

##### 4.2. Piston Flow Model (PFM)

In the *piston flow model* (PFM) approximation it is assumed that there are no flow lines with different transit times, and the hydrodynamic dispersion as well as molecular diffusion of the tracer are negligible. Thus the tracer moves from the recharge area as if it were in a parcel. The weighting function is given by the Dirac delta function [ $g(t') = \delta(t'-t_t)$ ], which inserted into Eq. 9 gives:

$$C(t) = C_{in}(t-t_t) \exp(-\lambda t_t) \quad (12)$$

Equation 12 means that the tracer which entered at a given time  $t-t_t$  leaves the system at the moment  $t$  with concentration decreased by the radio-

active decay during the time span  $t_t$ . The mean transit time of tracer ( $t_t$ ) equal to the mean transit time of water ( $t_w$ ) is the only parameter of PFM. Cases in which  $t_t$  may differ from  $t_w$  are discussed in Sect. 9.

#### 4.3. Exponential Model (EM)

In the *exponential model* (EM) approximation it is assumed that the exponential distribution of transit times exists, i.e., the shortest line has the transit time of zero and the longest line has the transit time of infinity. Tracer concentration for an instantaneous injection is:  $C_I(t) = C_I(0) \exp(-t/t_t)$ . This equation inserted into Eq. 9, and normalized in such a way that the initial concentration is as if the injected mass (M) was diluted in the volume of the system ( $V_m$ ), gives:

$$g(t') = t_t^{-1} \exp(-t'/t_t) \quad (13)$$

The mean transit time of tracer ( $t_t$ ) is the only parameter of EM. The exponential model is mathematically equivalent to the well known model of good mixing which is applicable to some lakes and industrial vessels. A lot of misunderstandings result from that property. Some investigators reject the exponential model because there is no possibility of good mixing in aquifers whereas others claim that the applicability of the model indicates conditions for a good mixing in the aquifer. Both approaches are wrong because the model is based on an assumption that no exchange (mixing) of tracer takes place between the flow lines [1, 6, 8]. The mixing takes place only at the sampling site (spring, river or abstraction well). That problem will be discussed further.

A normalized weighting function for EM is given in Fig. 1. Note that the normalization allows to represent an infinite number of cases by a single curve. In order to obtain the weighting function in real time it is necessary to assume a chosen value of  $t_t$  and recalculate the curve from Fig. 1.

The mean transit time of tracer ( $t_t$ ) equal to the mean transit time of water ( $t_w$ ) is the only parameter of EM. Cases in which  $t_t$  may differ from  $t_w$  are discussed in Sect. 9.

#### 4.4. Linear Model (LM)

In the *linear model* (LM) approximation it is assumed that the distribution of transit times is constant, i.e., all the flow lines have the same velocity but linearly increasing flow time. Similarly to EM, there is no mixing between the flow lines. The mixed sample is taken in a spring, river, or abstraction well [1, 3, 6]. The weighting function is:

$$\begin{aligned} g(t) &= 1/(2t_t) && \text{for } t' \leq 2t_t \\ &= 0 && \text{for } t' \geq 2t_t \end{aligned} \quad (14)$$

The mean transit time of tracer ( $t_t$ ) is the only parameter of LM. A normalized weighting function is given in Fig. 2. In order to obtain the weighting function in real time it is necessary to assume a chosen value of  $t_t$  and recalculate the curve from Fig. 2.



The mean transit time of tracer ( $t_t$ ) equal to the mean transit time of water ( $t_w$ ) is the only parameter of LM. Cases in which  $t_t$  may differ from  $t_w$  are discussed in Sect. 9.

#### 4.5. Combined Exponential-Piston Flow Model (EPM)

In general it is unrealistic to expect that single-parameter models can adequately describe real systems, and, therefore, a little more realistic two-parameter models have also been introduced. In the *exponential-piston model* it is assumed that the aquifer consists of two parts in line, one with the exponential distribution of transit times, and another with the distribution approximated by the piston flow. The weighting function of this model is [3, 6]:

$$g(t') = \begin{cases} (\eta/t_t) \exp(-\eta t'/t_t + \eta - 1) & \text{for } t' \geq t_t(1 - \eta^{-1}) \\ 0 & \text{for } t' \leq t_t(1 - \eta^{-1}) \end{cases} \quad (15)$$

where  $\eta$  is the ratio of the total volume to the volume with the exponential distribution of transit times, i.e.,  $\eta = 1$  means the exponential flow model (EM). The model has two fitting (sought) parameters,  $t_t$  and  $\eta$ . The weighting function does not depend on the order in which EM and PFM are combined. An example of a normalized weighting function obtained for  $\eta = 1.5$  is given in Fig. 1. However, experience shows that EPM works well for  $\eta$  values slightly larger than 1, e.i., for a dominating exponential flow pattern corrected for the presence of a small piston flow reservoir. In other cases, DM is more adequate.

In order to obtain the weighting function for a given value of  $\eta$  and a chosen  $t_t$  value in real time it is necessary to recalculate the curve from Fig. 1. Cases in which  $t_t$  may differ from  $t_w$  are discussed in Sect. 9.

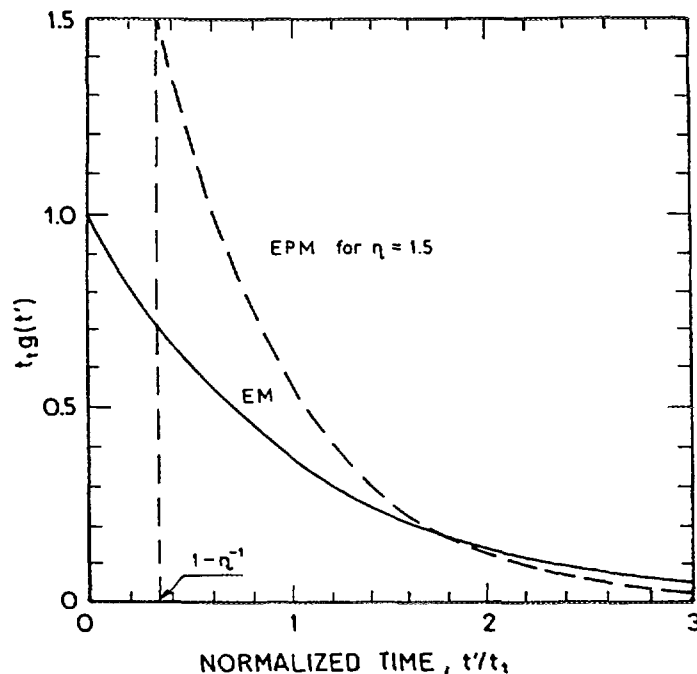


Fig. 1. The  $g(t')$  function of EM, and the  $g(t')$  function of EPM in the case of  $\eta = 1.5$  [3, 6].

#### 4.6. Combined Linear-Piston Flow Model (LPM)

The combination of LM with PFM gives similarly to EPM the *linear-piston model* (LPM). Similarly to EPM the weighting function has two parameters and does not depend on the order in which the models are combined. The weighting function is [3, 6]:

$$g(t') = \eta/(2t_t) \quad \text{for } t_t - t_t/\eta \leq t' \leq t_t + t_t/\eta \quad (16)$$

$$= 0 \quad \text{for other } t'$$

where  $\eta$  is the ratio of the total volume to the volume in which linear flow model applies, i.e.,  $\eta = 1.0$  means the linear flow model (LM). An example of the weighting function is given in Fig. 2. Weighting functions in real time are obtainable in the same way as described above for other models. Cases in which  $t_t$  differs from  $t_w$  are discussed in Sect. 9.

#### 4.7. Dispersion Model (DM)

In the *dispersion model* (DM) the uni-dimensional solution to the dispersion equation for a semi-infinite medium and flux injection-detection mode, developed in [20] and fully explained in [18], is usually put into Eq. 9 to obtain the weighting function, though sometimes other approximations are also applied. That weighting function reads [3, 6]:

$$g(t') = (4\pi t'^3/Pet_t)^{-1/2} \exp[-(1 - t'/t_t)^2 t_t Pe/t'] \quad (17)$$

where  $Pe$  is the so-called Peclet number. The reciprocal of  $Pe$  is equal to the dispersion parameter,  $Pe^{-1} = D/vx$ , where  $D$  is the dispersion coefficient. In the lumped parameter approach the dispersion parameter is treated as a single parameter. The meaning of that parameter is discussed in Sect. 9.1.

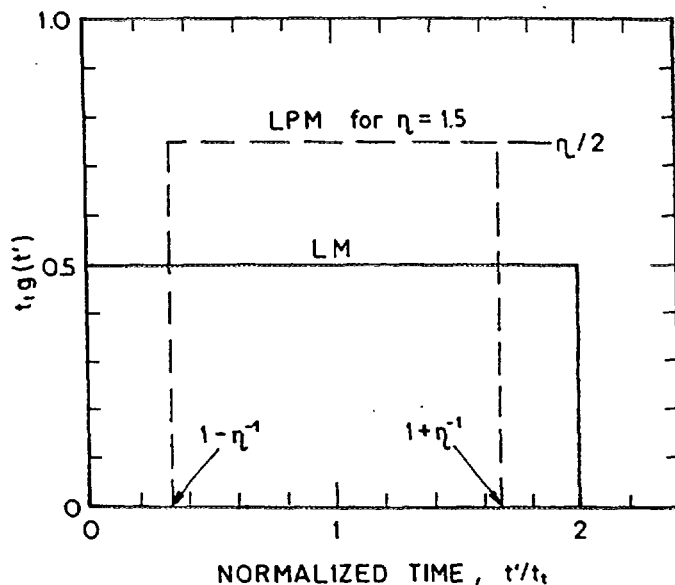


Fig. 2. The  $g(t')$  function of LM, and the  $g(t')$  function of LPM in the case of  $\eta = 1.5$  [3, 6].

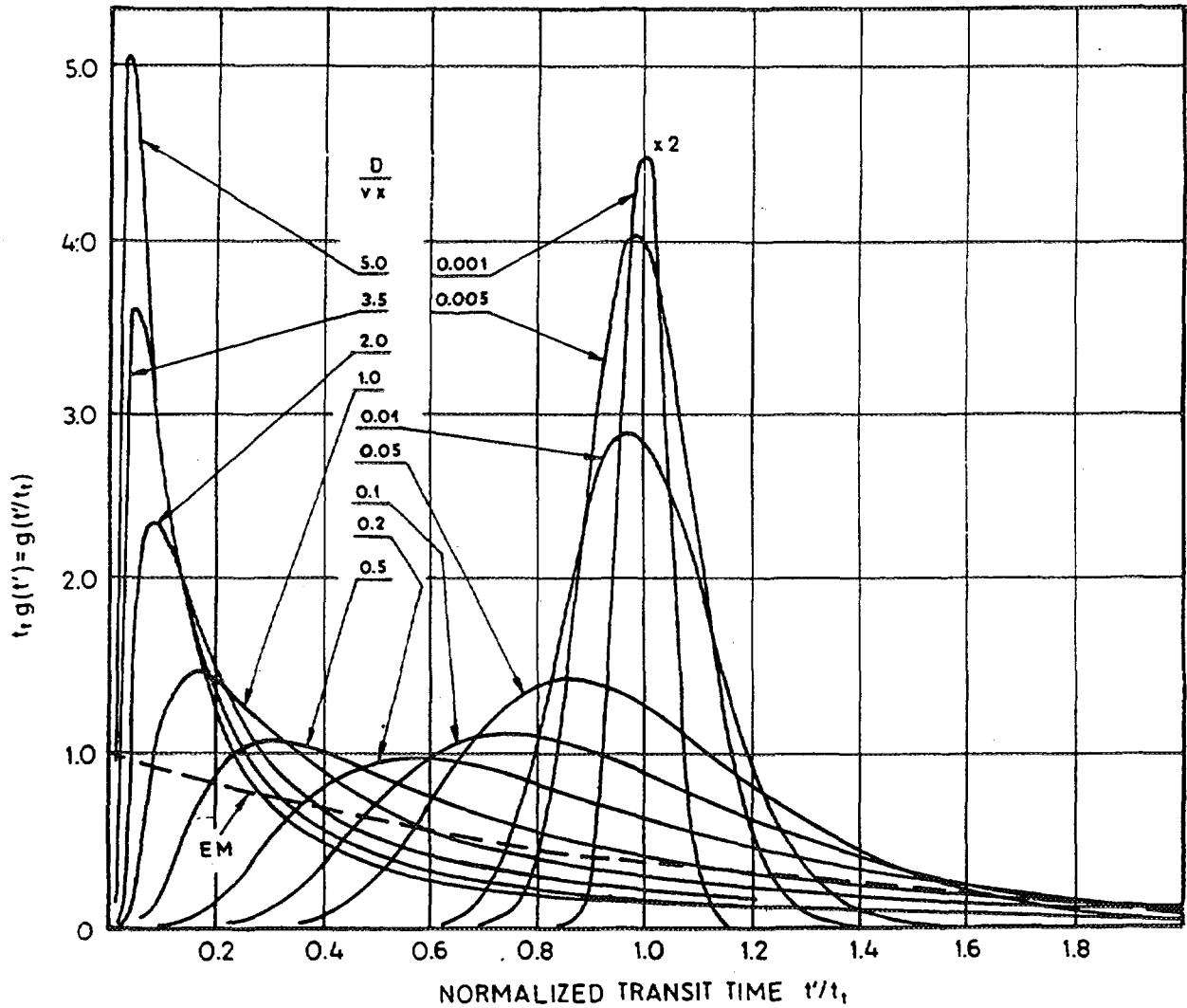


Fig. 3. Examples of the  $g(t')$  functions for DM in flux mode [3, 6]. The  $g(t')$  function of EM is shown for comparison.

Examples of normalized weighting functions for DM in the flux mode are shown in Fig. 3. Weighting functions in real time are obtainable in the same way as described above for other models. Cases in which  $t_t$  differs from  $t_w$  are discussed in Sect. 9.

The dispersion model can also be applied for the detection performed in the resident concentration mode (see Eq. 1). Then the weighting function reads [3, 6]:

$$g(t') = \left\{ \left( \frac{t'}{t_w} \right)^{-1/2} \exp \left[ - \left( 1 - \frac{t'}{t_w} \right)^2 \frac{t_w}{t'} \text{Pe} \right] - \left( \frac{\text{Pe}}{2} \right) \exp(\text{Pe}) \text{erfc} \left[ \left( 1 + \frac{t'}{t_w} \right) \left( \frac{4t'}{\text{Pe} t_w} \right)^{-1/2} \right] \right\} / t_w \quad (18)$$

where  $\text{erfc}(z) = 1 - \text{erf}(z)$ ,  $\text{erf}(z)$  being the tabulated error function. In the case of Eq. 18 the mean transit time of tracer always differs from the mean transit time of tracer and in ideal cases is given by:  $t_t = (1 + \text{Pe}^{-1})t_w$ , which shows that even if there are no stagnant zones in the system

the mean transit time of a conservative tracer may differ from the mean transit time of water. Cases of stagnant water zones are discussed in Sects 9.2 and 9.3.

A misunderstanding is possible as a result of different applications of the dispersion equation and its solutions. For instance, in the pollutant movement studies the dispersion equation usually serves as a distributed parameter model, especially when numerical solutions are used. Then, the dispersion coefficient (or the dispersivity,  $D/v$ , or dispersion parameter,  $Pe^{-1}$ , depending on the way in which the solutions are presented) represents the dispersive properties of the rock. If the dispersion model is used in the lumped parameter approach for the interpretation of environmental data in aquifers, the dispersion parameter is an apparent quantity which mainly depends on the distribution of flow transit times, and is practically order of magnitudes larger than the dispersion parameter resulting from the hydrodynamic dispersion, as explained in Sect. 9.1. However, in the studies of vertical movement through the unsaturated zone, or in some cases of river bank infiltration, the dispersion parameter can be related the hydrodynamic dispersion.

## 5. Cases of constant tracer input

For radioisotope tracers, the cases of a constant input can be solved analytically. They are applicable mainly to  $^{14}C$  and tritium prior to atmospheric fusion-bomb tests in the early 1950s. The following solutions are obtainable from Eq. 9 [1, 3, 6]:

$$C = C_0 \exp(-\lambda/t_a) \quad \text{for PFM} \quad (19)$$

$$C = C_0 / (1 + \lambda/t_a) \quad \text{for EM} \quad (20)$$

$$C = C_0 [1 - \exp(-2\lambda t_a)] / (2\lambda t_a) \quad \text{for LM} \quad (21)$$

$$C = C_0 \exp\{(Pe/2) \times [1 - (1 + 4\lambda t_a Pe^{-1})^{1/2}]\} \quad \text{for DM} \quad (22)$$

where  $C_0$  is a constant concentration measured in water entering the system and  $t_w$  is replaced by  $t_a$  (radioisotope age) to the reasons discussed in detail in Sect. 9. Here, we shall remind only that for nonsorbable tracers and systems without stagnant zones  $t_w = t_a$ . Unfortunately, it is a common mistake to identify the radiocarbon age obtained from Eq. 19 with the water age without any information if PFM is applicable and if the radiocarbon is not delayed by interaction between dissolved and solid carbonates.

Relative concentration ( $C/C_0$ ) given as functions of normalized time ( $\lambda t_a$ ) are given in Fig. 4 (for tritium  $1/\lambda = 17.9$  a, and for radiocarbon  $1/\lambda = 8,300$  a). From Eqs 19 to 22 and Fig. 4, several conclusions can immediately be drawn. First, for a sample taken from a well, it is in principle not possible to distinguish if the system is mobile or immobile (however, if a short-lived radioisotope is present, it would be unreasonable to assume that the system can be separated from the recharge). Second, the applicability of the piston flow model (PFM) is justified for a constant tracer input to systems with the values of the dispersion parameter, say, not larger than about 0.05. Third, from the measured  $C/C_0$  ratio it is not possible to obtain the radioisotope age without the knowledge on the model of flow pattern even if a single-parameter model is assumed. Fourth, for ages below, say,  $0.5(1/\lambda)$ ,

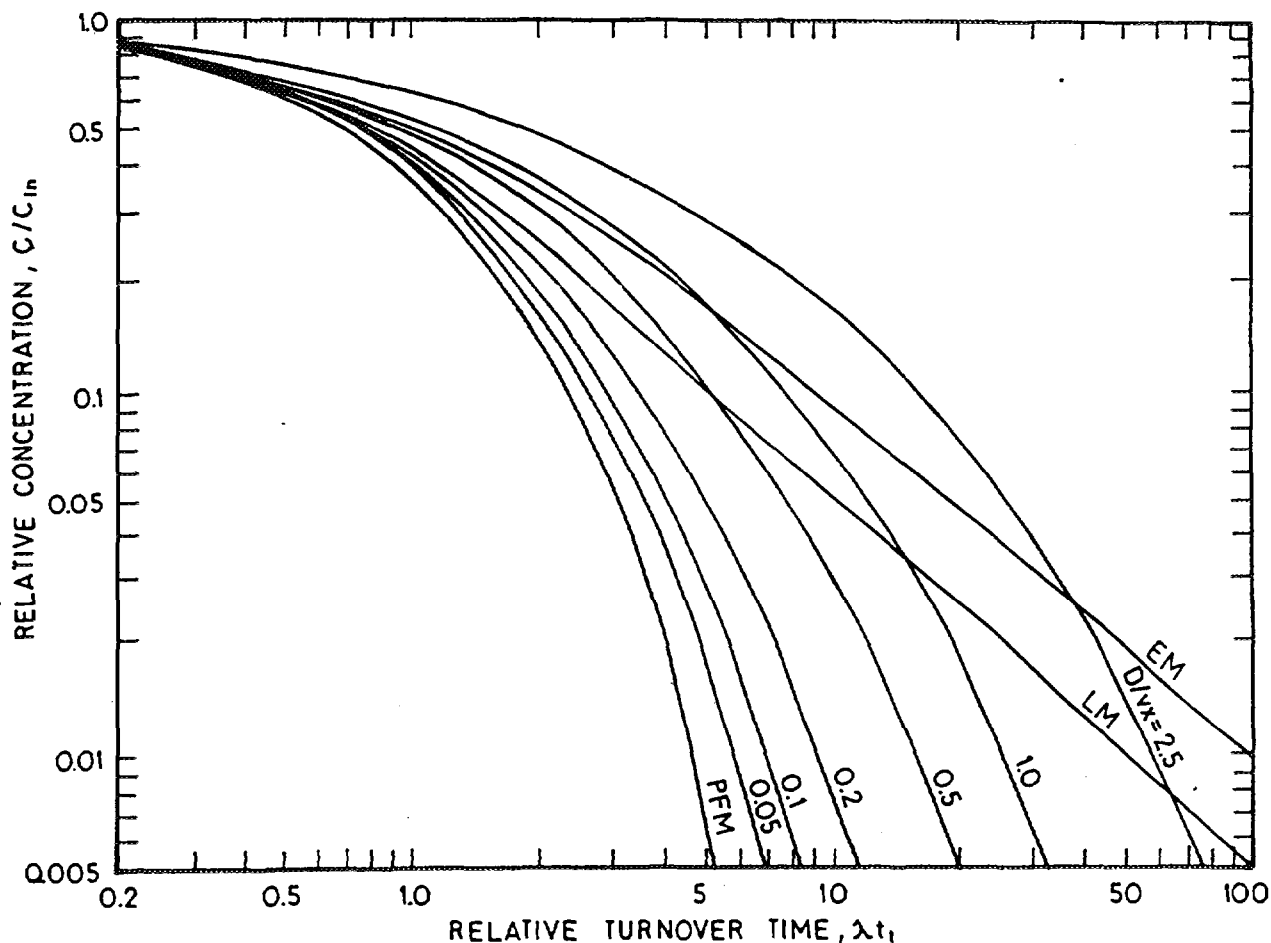


Fig. 4. Relative concentration versus relative radioisotope age ( $\lambda t_t$ ), in the case of a constant input of a radioactive tracer [3, 6]. EM - exponential model, LM - linear model, PFM - piston flow model,  $Pe^{-1}$  - dispersion parameter for the dispersion model in the flux mode.

the flow pattern (type of model) has low influence on the age obtained. Fifth, for two-parameter models it is impossible to obtain the age value (it is like solving a single equation with two unknowns).

When no information is available on the flow pattern, the ages obtained from PFM and EM can serve as brackets for real values, though in some extreme cases DM can yield higher ages (see Fig. 4).

Radioisotopes with a constant input are applicable as tracers for the age determination due to the existence of a sink (radioactive decay), which is adherent to the sought parameter (see the definition of an ideal tracer in Sect. 1.2). Other substances cannot serve as tracers for this purpose though they come under earlier definitions of an ideal tracer. However, those other substances (e.g.,  $Cl^-$ ) may serve as good tracers for other purposes, e.g., for determining the mixing ratio of different waters.

Note that for a constant tracer input, a single determination serves for the calculation of age. Therefore, no calibration can be performed. The only way to validate, or confirm, a model is to compare its results with other independent data, if available.

## 6. Cases of variable tracer input

### 6.1. Tritium method

Seasonal variations of the tritium concentration in precipitation cause serious difficulties in calculating the input function,  $C_{in}(t)$ . The best method would be to estimate for each year the mean concentration weighted by the infiltration rates:

$$C_{in} = \frac{\sum_{i=1}^{12} C_i \alpha_i P_i}{\sum_{i=1}^{12} \alpha_i P_i} \quad (23)$$

where  $C_i$ ,  $\alpha_i$  and  $P_i$  are the  $^3\text{H}$  concentrations in precipitation, infiltration coefficients, and monthly precipitation amounts for  $i$ th month, respectively.  $C_i$  is to be taken from the nearest IAEA network station, and for early time periods by correlations between that station and other stations for which long records are available [2]. The precipitation rates are to be taken from the nearest meteorologic station, or as the mean of two or three stations if the supposed recharge area lies between them. Usually, it is assumed that the infiltration coefficient in the summer months ( $\alpha_s$ ) is only a given fraction ( $\alpha$ ) of the winter coefficient ( $\alpha_w$ ). Then, Eq. 23 simplifies to:

$$C_{in} = [(\alpha \sum_i P_i)_s + (\sum_i P_i)_w] / [(\alpha \sum_i P_i)_s + (\sum_i P_i)_w] \quad (24)$$

where subscripts "s" and "w" mean the summing over the summer and winter months, respectively. For the northern hemisphere, the summer months are from April to September and winter months from October to March, and the same  $\alpha$  value is assumed for each year.

The input function is constructed by applying Eq. 24 to the known  $C_i$  and  $P_i$  data of each year, and for an assumed  $\alpha$  value. In some cases Eq. 23 is applied if there is no surface run-off and  $\alpha_i$  coefficients can be found from the actual evapotranspiration and precipitation data. The actual evapotranspiration is either estimated from pan-evaporimeter experiments [21] or by the use of an empirical formula for the potential evapotranspiration [22]. Monthly precipitation has to be measured in the recharge area, or can be taken from a nearby station. Monthly  $^3\text{H}$  concentrations in precipitation are known from publications of the IAEA [23] by taking data for the nearest station or by applying correlated data of other stations [2].

It is well known that under moderate climatic conditions the recharge of aquifers takes place mainly in winter and early spring. Consequently, in early publications on the tritium input function, the summer infiltration was either completely neglected [2], or  $\alpha$  was taken as equal 0.05 [3, 6]. Similar opinion on the tritium input function was expressed in a recent review of the dating methods for young groundwaters [4]. However, whenever the stable isotopic composition of groundwater reflects that of the average precipitation there is no reason to reject the influence of summer tritium input. This is because even if no net recharge takes place in summer months, the water which reaches the water table in winter months is usually a mixture of both winter and summer water. Otherwise the stable isotopic composition of groundwater would reflect only the winter and early spring precipitation, which is not the case, as observed in many areas of the world, and as discussed below for two case studies in Poland.

Rearranged Eq. 24 can be used in an opposite way in order to find the  $\alpha$  value [24]:

$$\alpha = \frac{[\sum_i (P_i C_i)_w - C] \sum_i (P_i)_w}{[C - \sum_i (P_i C_i)_s] \sum_i (P_i)_s} \quad (25)$$

where  $C$  stays for the mean values of  $\delta^{18}\text{O}$  or  $\delta\text{D}$  of the local groundwater originating from the modern precipitation, and  $C_i$  represents mean monthly values in precipitation. Theoretically, the summings in Eq. 25 should be performed for the whole time period which contribute to the formation of water in a given underground system. Unfortunately, this time period is unknown prior to the tritium interpretation. Much more serious limitation results from the lack of sufficient records of stable isotope content in precipitation. Therefore, the longer the record of stable isotope content in precipitation, the better the approximation. For a seven year record in Cracow station, and for typical groundwaters in the area, it was found that the  $\alpha$  value is about 0.6-0.7, and that the values of model parameters found by calibration slightly depend on the assumed  $\alpha$  value in the range of 0.4 to 1.0 (see case studies in Ruszcza and Czatkowice described in Sects 10.1 and 10.2). Therefore, whenever the mean isotopic composition of groundwater is close to that of the precipitation, it is advised to use  $\alpha = 0.5$  to 0.7. Such situations are typically observed under moderate climatic conditions and in tropical humid areas (e.g. in the Amazonia basin). In other areas the tritium input function cannot be found so easily.

Note that unless the input function is found independently, the  $\alpha$  parameter is either arbitrarily assumed by the modeller, or tacitly used as hidden fitting parameter (see Sects 10.1 and 10.2 for case studies in which  $\alpha$  was used as a fitting parameter in an explicit way).

## 6.2. Tritium-helium method

As the tritium peak in the atmosphere, which was caused by hydrogen bomb test, passes and  $^3\text{H}$  concentration in groundwaters declines slowly approaching the pre-bomb era values, the interest of a number of researchers has been directed to other methods covering similar range of ages. In the  $^3\text{H}$ - $^3\text{He}$  method either the ratio of tritiogenic  $^3\text{He}$  to  $^3\text{H}$  is considered, or theoretical contents of both tracers are fitted (calibration process) to the observation data independently [4, 6, 25-31]. The method has several advantages and disadvantages. In order to measure  $^3\text{He}$  a costly mass-spectrometer is needed and additional sources and sinks of  $^3\text{He}$  in groundwater must be taken into account. The main advantage seemed to result from the  $^3\text{He}/^3\text{H}$  peak to appear much later in groundwater systems than the  $^3\text{H}$  peak of 1963. Unfortunately, in some early estimates of the potential abilities of that method, the influence of a low accuracy of the ratio for low tritium contents was not taken into account.

Another advantage consists in the  $^3\text{He}/^3\text{H}$  ratio being independent of the initial tritium content for the piston flow model (PFM). Then the tracer age is:

$$t_t = \lambda_T^{-1} \ln[1 + ^3\text{He}_T/^3\text{H}] \quad (26)$$

where  $\lambda_T$  is the radioactive decay constant for tritium ( $\lambda_T^{-1} = t_{1/2}/\ln 2 = 12.4/0.693 = 17.9$  a), and  $^3\text{He}_T$  stays for tritiogenic  $^3\text{He}$  content expressed in T.U. (for  $^3\text{He}$  expressed in ml STP of gas per gram of water, the factor is  $4.01 \times 10^{14}$  to obtain the  $^3\text{He}$  content in T.U.).

Unfortunately, contrary to the statements of some authors, Eq. 26 does not apply to other flow models. In general, the following equations have to be considered [31]:

$$C_T(t) = \int_0^{\infty} C_{Tin}(t-t') g(t') \exp(-\lambda t') dt' \quad (27)$$

for tritium, and

$$C_{He}(t) = \int_0^{\infty} C_{Tin}(t-t') g(t') [1 - \exp(-\lambda t')] dt' \quad (28)$$

for the daughter  $^3\text{He}$ . From these equations, and from examples of theoretical concentrations curves (solutions to the direct problem) given in [31], it is clear that the results of the  $^3\text{H}$ - $^3\text{He}$  method depend on the tritium input function.

Several recent case studies show that in vertical transport through the unsaturated zone, or for horizontal flow in the saturated zone, when the particular flow paths can be observed by multi-level samplers, the  $^3\text{H}$ - $^3\text{He}$  method in the piston flow approximation yields satisfactory or acceptable results [27-30]. However, for typical applications of the lumped-parameter approach, when Eqs 27 and 28 must be used, and where possible sources and sinks of  $^3\text{He}$  influence the concentrations measured, the  $^3\text{H}$ - $^3\text{He}$  method does not seem to yield similar ages as the tritium method [32]. The main sources and sinks result from possible gains and losses of  $^3\text{He}$  by diffusional exchange with the atmosphere, if the water is not well separated on its way after the recharge event.

### 6.3. Krypton-85 method

The  $^{85}\text{Kr}$  content in the atmosphere results from nuclear power stations and plutonium production for military purposes. Large scatter of observed concentrations shows that there are spatial and temporal variations of the  $^{85}\text{Kr}$  activity. However, yearly averages give relatively smooth input functions for both hemispheres [32-35]. The input function started from zero in early 1950s and monotonically reached about 750 dpm/mmol Kr in early 1980s. The  $^{85}\text{Kr}$  concentration is expressed in Kr dissolved in water by equilibration with the atmosphere, and, therefore it does not depend on the temperature at the recharge area, though the concentration of Kr is temperature dependent. Initially, it was hoped that the  $^{85}\text{Kr}$  method would replace the tritium method [36] when the tritium peak disappears. However, due to large samples required and a low accuracy, the method is very seldom applied, though, similarly to the  $^3\text{H}$ - $^3\text{He}$  method, a successful application for determining the water age along flow paths is known [37]. In spite of the present limitations of the  $^{85}\text{Kr}$  method, it is, together with man-made volatile organic compounds discussed in Sect. 6.6, one of the most promising methods for future dating of young groundwaters [4], though similar limitations as in the case of the  $^3\text{H}$ - $^3\text{He}$  method can be expected due to possible diffusional losses or gains [32].

The solutions to the direct problem given in [6] indicate that for short transit times (ages), say, of the order of 5 years, the differences between particular models are slight, similarly as for constant tracer input (see Sect. 5). For longer transit times, the differences become larger, and, contrary to the statements of some authors, long records are needed to differentiate responses of particular models.



#### 6.4. Carbon-14 method as a variable input tracer

Usually the  $^{14}\text{C}$  content is not measured in young waters in which tritium is present unless mixing of waters having distinctly different ages is to be investigated. However, in principle, the variable  $^{14}\text{C}$  concentrations of the bomb era can also be interpreted by the lumped-parameter approach, though the method is costly and the accuracy limited due to the problems related to the so-called initial carbon content [38, 39]. Therefore, it is possible only to check if the carbon data are consistent with the model obtained from the tritium interpretation [6, 32].

#### 6.5. Oxygen-18 and/or deuterium method

Seasonal variations of  $\delta^{18}\text{O}$  and  $\delta\text{D}$  in precipitation are known to be also observable in small systems with the mean transit time up to about 4 years, though with a strong damping. Several successful applications of the lumped parameter approach to such systems with  $^{18}\text{O}$  and D as tracers are known. In order to obtain a representative output concentration curve, a frequent sampling is needed, and a several year record of precipitation and stable isotope data from a nearby meteorologic station. The method proposed in [40, 41] for finding the input function, is also included in the FLOW program within the present manual. The input function is found from the following formula (where C stays for delta values of  $^{18}\text{O}$  or D):

$$C_{in}(t) = \bar{C} + [N\alpha_i P_i (C_i - \bar{C})] / \sum_i \alpha_i P_i \quad (29)$$

where  $\bar{C}$  is the mean output concentration, and N is the number of months (or weeks, or two-week periods) for which observations are available. Usually, instead of monthly infiltration rates ( $\alpha_i$ ), the coefficient  $\alpha$  given by Eq. 25 is used. For small retention basins the  $\alpha$  coefficient can also be estimated from the hydrologic data as  $(Q_s/P_s)/(Q_w/P_w)$ , where  $Q_s$  and  $Q_w$  are the summer and winter outflows from the basin, respectively [40, 41]. The Wimbachtal Valley case study showed that the values of the  $\alpha$  coefficient determined by these two methods may differ considerably when the snow cover accumulated in winter months melts in summer months.

#### 6.6. Other methods

Among other variable tracers which are the most promising for dating the young groundwaters are freon-12 ( $\text{CCl}_2\text{F}_2$ ) and  $\text{SF}_6$ . In 1970s a number of authors demonstrated the applicability of chlorofluorocarbons (mainly freon-11) to trace the movement of sewage in groundwaters [4]. However, early attempts of dating with freon-11 by the lumped-parameter approach were not very successful [32], most probably due to the adsorption of that tracer and exchange with the atmosphere. However, conclusions reached in several recent publications indicate that freon-11 and freon-12 are in general applicable to trace young waters [4, 42, 43]. In a case study in Maryland a number of sampling wells were installed with screens only 0.9 m long [43]. Therefore, it was possible to use the piston flow approximation (advective transport only) for determining the freon-11 and freon-12 ages which were next used to calibrate a numerical flow and transport model. However, in our opinion, no good fit was obtained for these two tracers, and for the tritium tracer (interpreted both by the advective model and numerical dispersion model), though the conclusion reached was that the calibration was reason-

bly good. In spite of difficulties encountered with gaseous tracers, some of the man-made gases with monotonically increasing atmospheric concentrations can be considered as promising for dating of young waters, and, therefore, an adequate option is included in the FLOW program mentioned earlier.

Most probably, SF<sub>6</sub> should also be included to the list of promising environmental tracers for groundwater dating [44].

Though technical difficulties with contamination of samples have been overcome [4], still some limitations for dating with all gaseous tracers discussed within this section result from the dependence of their solubility on the temperature at the recharge area, and on possible contamination of groundwater by local pollution sources [4]. The modelling problems are similar as those discussed for <sup>85</sup>Kr in Sect. 6.3 with additional difficulties mentioned above.

### 6.7. Goodness of fit

In the case of variable tracer input, the model is usually fitted (calibrated) to the set of observation data. The goodness of fit is within the present manual given by SIGMA defined as:

$$\text{SIGMA} = \left[ \sum_{i=1}^n (C_{m_i} - C_i)^2 \right]^{1/2} / n \quad (30)$$

where  $C_{m_i}$  is the  $i$ th measured concentration,  $C_i$  is the  $i$ th calculated concentration and  $n$  is the number of observations.

## 7. Other models related to the lumped-parameter approach

A number of models have been derived from the piston flow model with a constant input, which take into account possible underground production of the tracer, its interactions with the solid phase, dilution, enrichment due to membrane filtration (ultrafiltration) and diffusion exchange with aquicludes or aquitards. These models mainly serve for the interpretation of such radioisotopes as <sup>14</sup>C in a steady state, <sup>36</sup>Cl, <sup>234</sup>U/<sup>238</sup>U, and others. Their review is far beyond the scope of the present manual. References to a number of papers devoted to these models can be found in [8].

## 8. Variable flow

Groundwater systems are never constant, thus the assumption of a constant flow rate seems to be unjustified. Therefore, there were a number of attempts to solve the problem of variable flow in the lumped-parameter approach. It has been shown that Eq. 11 results from a more general formula in which the flux of tracer, i.e., the product  $C(t) \times Q(t)$  is convoluted, and the weighting function is defined for the flux [45]. Therefore, it is evident that to interpret the tracer data in variable flow, the records of input and output flow rates are also needed. In some cases, from the record of the outflow rate it is possible to calculate the inflow rate, and to perform the interpretation of tracer data [45, 46]. In a study of a small retention basin (0.76 km<sup>2</sup>) with a high changes in flow rate, the variable flow approach was shown to yield slightly better fit, but the mean turnover time was very close to that found from the steady-state approach [46]. Therefore, it was concluded that when the variable part of the investigated system is small in comparison with the total volume of the system, the steady state approxima-

tion is applicable. Most probably the majority of groundwater systems satisfy well this condition. Intuitively, changes in the volume and flow rates should also be short in comparison with the duration of changes in tracer concentration and its half-life time in case of radioisotopes. Under these conditions, the steady-state approach should yield satisfactory results.

## 9. Relations between model parameters and flow parameters

### 9.1. Applicability of the models

In principle, the distribution of flow lines within the investigated system is not considered in the lumped-parameter approach. However, in the interpretation of environmental tracer data, where records of data are usually too short to select the most adequate model only by calibration, selection of models can be performed on the basis of available geological or technical information. Such a selection can be performed either prior to calibration or after the calibration of several models. Fig. 5 presents several typical situations to which particular models are applicable.

The piston flow model (PFM) may be used to situations shown in the first part of Fig. 5 under the following conditions: (1) the length of the recharge zone measured in the direction of flow is negligible in comparison with the distance to the sampling site, (2) the aquifer is sufficiently homogeneous to have similar velocities in a given vertical cross-section, (3) the input concentration should either be constant or monotonically slowly changing, and (4) for a radioisotope tracer, its half-life time should preferably be lower than the age of water. These conditions are mostly intuitive, but examples given in Fig. 4 demonstrate how PFM compares with other models for a constant radioisotope tracer input. Examples of direct solutions for  $^{85}\text{Kr}$  tracer and different models can be found in [6]. In spite of all its drawbacks, PFM may be convenient for fast and easy estimations.

The piston flow model can also be used in other situations shown in Fig. 5 if a small fraction of a well is screened, which gives a situation similar to that shown in cross-section 1.

The exponential model can be used for situations shown as a, b, and d in cross-section 2 of Fig. 5 providing the transit time through the unsaturated zone is negligible in comparison with the total transit time. This condition results from the shape of the weighting function (Fig. 2) in which the infinitesimally short transit time appears. It is a common mistake to fit EM to the data obtained on samples taken at a great depth, or from an artesian well, or even from a phreatic aquifer but with a thick unsaturated zone. In all such cases the extremely short transit times do not exist, and, consequently, EM is not applicable.

If the transit time through the unsaturated zone is not negligible, or if the abstraction well is screened at a certain depth (see case c in cross-section 2, Fig. 5), or finally if the aquifer is partly confined (cross-section 3, Fig. 5), the exponential-piston model and alternatively the dispersion model are applicable.

As mentioned, for the piston flow model no dispersion is allowed and all the flow lines have the same transit time. For the exponential and linear models and for their combinations with the piston flow model (EPM and LPM, respectively), no exchange of tracer between flow lines is assumed. For the dispersion model (DM), no assumption is needed on the dispersivity. However, one should keep in mind that in most cases, the apparent dispersivity results from the distribution of transit times of particular flow lines. In an extreme case (e.g., d in cross-section 2, Fig. 5, which can be equivalent to the exponential flow case) the mean distance from the recharge area to the drainage point is  $x = 0.5x_0$ , where  $x_0$  is the length of the recharge zone measured along the direction of flow. Then, the recharge

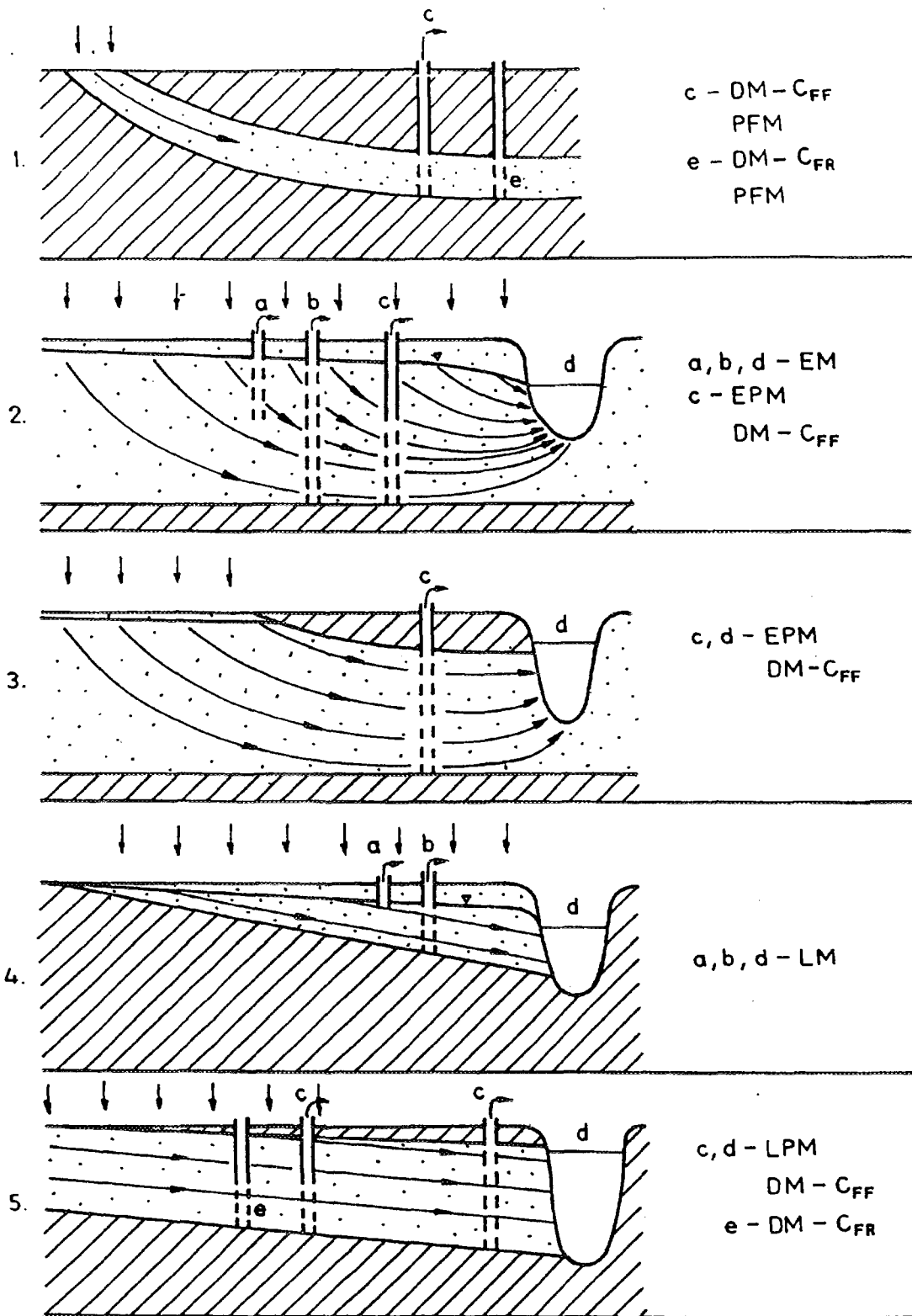


Fig. 5. Schematic situations showing examples of possible applicability of models [3, 6]. Cases a, b, c, and d correspond to sampling in outflowing or abstracted water (the sampling is averaged by the flow rates,  $C_{FF}$  mode).

Case e corresponds to samples taken separately at different depths and next averaged by the depth intervals ( $C_{FR}$  mode).

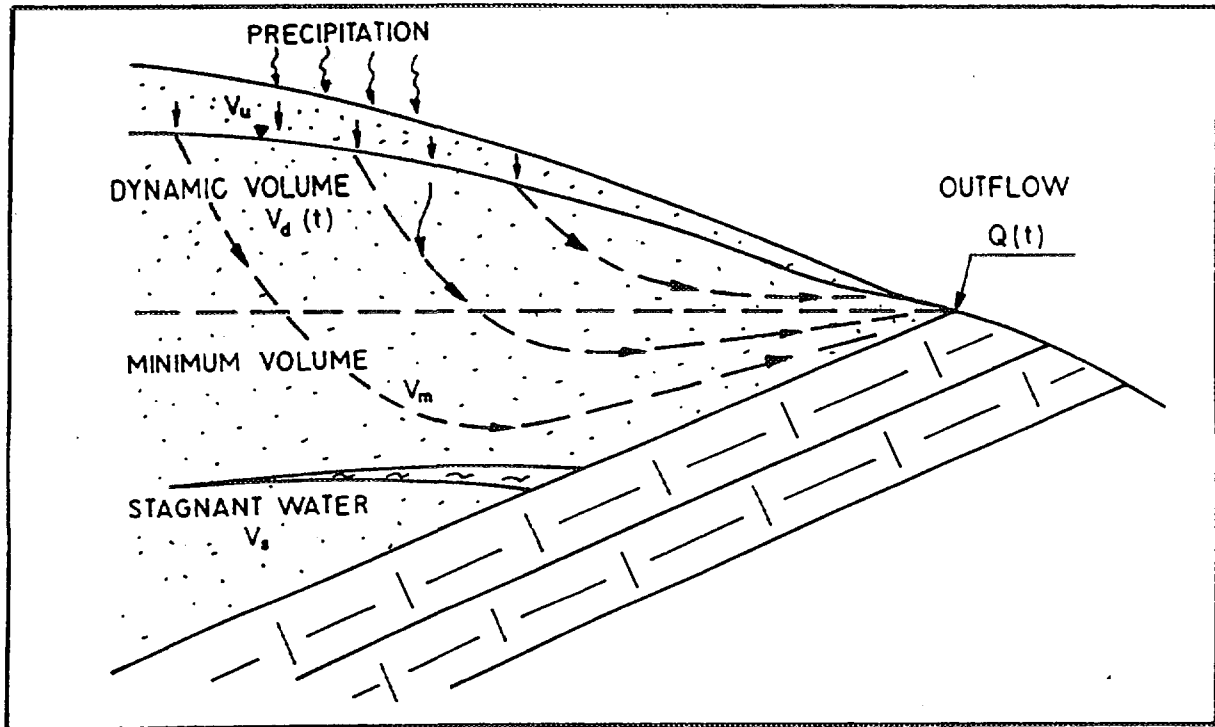


Fig. 6. Schematic presentation of different parts of a groundwater system in relation to the concept of tracer age in the lumped-parameter approach [45].

$V_u$  - volume of water in the unsaturated zone,  $V_d$  - dynamic volume which influences the outflow rate,  $Q$ ,  $V_{min}$  - minimum volume which is observed for periods in which  $Q = 0$ ,  $V_s$  - stagnant volume in a sedimentation pocket.

parameter should not exceed 2 because if  $D/v$  is the measure of heterogeneity, the dispersion parameter is:  $D/vx = x_0/x = 2$ . Somewhat similar conclusion can be reached from Fig. 4 for a constant tracer input. For low values of the relative age, the dispersion model with  $D/vx = 0.5$  is close to the exponential model. However, for higher values of the relative age, the dispersion model with  $D/vx = 2.5$  is the closest one to the exponential model (EM).

Note that if the samples are taken in the discharge area ( $d$ ) or in abstracted water ( $a$ ,  $b$ , or  $c$ ) the dispersion model in the flux mode is applicable (weighting function given by Eq. 17). However, if samples are taken at different depths of the well and the mean value is averaged over the sampled depth interval, Eq. 18 is applicable, because then the detection is in the resident mode (see Appendix A for graphical presentation of possible differences between the weighting functions).

### 9.2. Granular aquifers

In granular systems there is no difference between the conservative tracer age ( $t_t$ ) and the radioisotope age ( $t_a$ ), and, in principle, the tracer age is equal to the water age ( $t_w$ ). Therefore, when dealing with granular aquifers these different concepts of ages are not necessary. However, even for granular aquifers misunderstandings are possible in relation to the

meaning of parameters obtained from the interpretation of tracer data. In Fig. 6 a schematic presentation of possible flow and tracer paths through an aquifer is shown. The tracer age determined from the interpretation of tracer concentrations in the outflow will yield the total mobile water volume ( $V_m$ ) which is equal to the sum of water volume in the unsaturated zone ( $V_u$ ), the dynamic water volume ( $V_d$ ), and the minimum volume ( $V_{min}$ ). The stagnant water in a sedimentation pocket ( $V_s$ ) is neither included in the definition of water age (Eq. 3) nor it distinctly influences the tracer age, if the tracer diffusion is limited due to a small area of contact and a large extension of the pocket. It is evident from Fig. 6 that the dynamic volume which can be determined from the recession curve of the volumetric flow rate should not be identified with the mobile water volume. It is also evident that for some groundwater systems the transit time through the unsaturated zone is not negligible in comparison with the transit time in the saturated zone, and, therefore, the tracer age can be related to the aquifer parameters only if corrected for the transit time through the unsaturated zone (see Sect. 10.1).

A new abstraction well screened at the interval of a sedimentation pocket, like that shown in Fig. 6, will initially yield water with the tracer age much larger than that in the active part of the aquifer. If the pocket has large dimensions, the tracer data will not disclose for a long time that a connection with the active part exists, and a large tracer age may lead to the overestimation of the volume of that part of the investigated system. On the other hand, the tracer data from the active part of the system will lead to the underestimation of the total volume. Therefore, it can be expected that in highly heterogeneous systems the tracer ages obtained from the lumped-parameter approach will differ from the water ages. Numerical simulations performed with two-dimensional flow and transport models and compared with the interpretation performed with the aid of Eq. 11 confirmed that for highly heterogeneous systems the tracer age observed at the outlet is usually smaller than the water age [47].

### 9.3. Karstified and fractured aquifers

In fractured or karstified rocks the movement of water takes place mainly in fractures or in karstic channels whereas stagnant or quasi stagnant water in the microporous rock matrix is easily available to tracer by molecular diffusion. In such a case the tracer transport is delayed in respect to the mass transport of water (transport of mobile water) due to the additional time spent by the tracer in stagnant zone(s). The retardation factor caused by molecular diffusion exchange between the mobile water in fissures or channels and stagnant water in the matrix is given by the following formula [48, 49, 50]:

$$R_p = v_w/v_t = t_t/t_w = (V_p + V_f)/V_f = (n_p + n_f)/n_f - n_p \cong (n_p + n_f)/n_f \quad (31)$$

where ( $R_p$ ) is the retardation factor,  $n_p$  is the matrix porosity, and  $n_f$  is the fissure porosity (or more generally the mobile water porosity, usually called the effective porosity, and denoted in Eq. 4 as  $n_e$ ). Note that  $n_p$  is defined for a unit volume of the matrix whereas  $n_f$  is defined for a representative unit volume of the whole rock. Equation 31 was first derived for a model of the fissure network represented by parallel fissures of equal aperture and spacing, as shown in Fig. 7, and in Fig. 8 in the lumped approach.

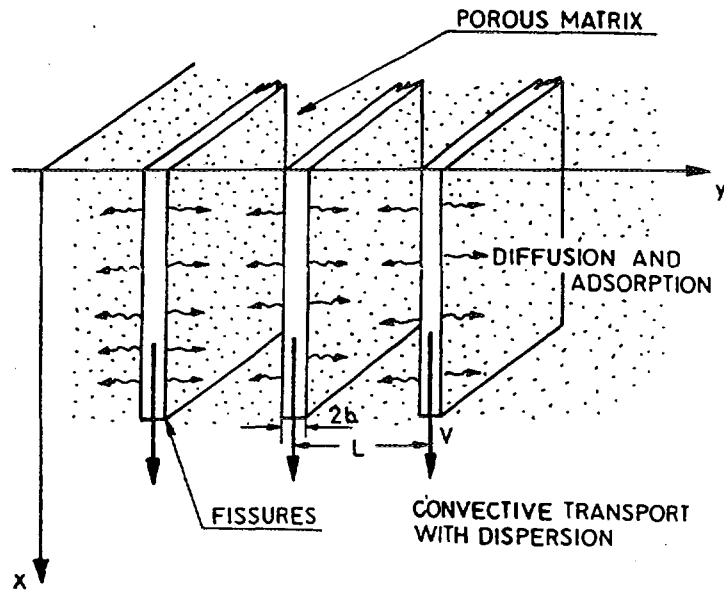


Fig. 7. A model of parallel fissure system with the exchange of tracer between the mobile water in fissures and stagnant water in the micropores.

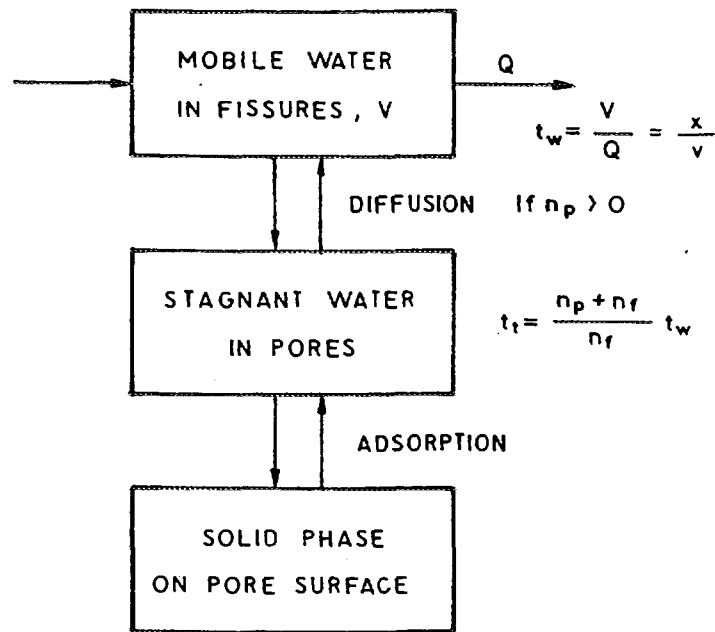


Fig. 8. A lumped-parameter approach to the system shown in Fig. 7. Note that  $t_w$  is not influenced by stagnant water volume whereas  $t_t$  is governed by matrix porosity, especially when  $n_p \gg n_f$  which is a common case.

It is evident from Eq. 31 that the retardation factor, i.e., the ratio of tracer age to the mean travel time of mobile water, is independent of the fissure network arrangement and the coefficient of matrix diffusion.

Equation 31 is theoretically applicable at any distance, however, in practice, its applicability is limited to large scales as discussed in [13]. The movement of environmental tracers is usually observed at large scales.

If  $v_w$  expressed by Eq. 31 is put into Eq. 4, one gets the following formula for Darcy's velocity [13, 19, 49]:

$$v_f = (n_p + n_f)v_t \cong n_p v_t = n_p (x/t_t) \quad (32)$$

which immediately gives the hydraulic conductivity:

$$k = (n_p + n_f)v_t / (\Delta H / \Delta x) \cong n_p v_t / (\Delta H / \Delta x) = n_p (x/t_t) / (\Delta H / \Delta x) \quad (33)$$

Comparison of Eqs 32 and 33 with Eq. 4 shows that if the tracer velocity is used instead of the mobile water velocity, the total open (accessible for tracer) porosity (i.e.  $n_p + n_f$ ) replaces the fissure porosity. However, the matrix porosity is seldom below 0.02 (2 %) whereas the fissure porosity is seldom above 0.001 (0.1 %), i.e.  $n_p \gg n_f$ . Carbonate rocks are often characterized by fissure porosities of about 0.01, but their matrix porosities are also higher (e.g., for chalks and marls about 0.3 to 0.4). Therefore, the fissure porosity can usually be neglected in a good approximation. Contrary to the fissure porosity, the matrix porosity is easily measurable on rock samples. Then, the approximate forms of Eqs 32 and 33 are applicable, which means that if either the tracer velocity or the tracer age is known, Darcy's velocity and the hydraulic conductivity can be estimated at large scale without any knowledge on the parameters of the fissure network, and vice versa, if the hydraulic conductivity is known (e.g. from pumping tests), the mean velocity of a conservative pollutant can be predicted. Even if the condition  $n_p \gg n_f$  is not well satisfied, the use of the approximate forms of Eqs 30 and 33 still seem to be better justified than the use of the effective porosity which is either defined as that in which the water flux occurs or undefined (some authors seem to define the effective porosity as that in which the tracer transport takes place, and at the same time to be equal to that in which the water movement takes place).

Some authors identify the specific yield with the effective porosity. However, for granular rocks the specific yield is always lower than the effective porosity defined for water flux, whereas for fissured rocks, the specific yield can be larger than the effective porosity. The identification of the effective porosity with the fissure porosity is an approximation because dead-end fissures may contain stagnant water (then  $n_e < n_f$ ), and in large micropores some movement of water may exist (then  $n_e > n_f$ ). In any case, for typical fissured rocks one can assume that  $n_e \cong n_f \ll n_p$ . For fissured rocks with the matrix characterized by large pores, the specific yield is larger than  $n_f$  and smaller than  $n_p$ .

It is evident from Eqs 31-33 that the solute time of travel is mainly governed by the largest water reservoir available for solute during its transport, although the solute enters and leaves the stagnant reservoir only by molecular diffusion. The mobile water reservoir in fissures is usually negligible for the estimation of the solute time of travel. In other words, the "effective porosity" applied by some workers for diffusible solutes must



be equal to the total porosity, or in approximation to the matrix porosity. However, it must be remembered, that the "effective porosity" defined for the solute transport differs from the effective porosity commonly applied in Darcy's law.

From Eq. 3 and 31 it follows that the total volume of water accessible to the tracer is [13]:

$$V = V_p + V_f = Qt_t \quad (34)$$

and the volume of rock ( $V_r$ ) is:

$$V_r = V/(n_f + n_p) = Qt_t/(n_f + n_p) \cong Qt_t/n_p \quad (35)$$

It follows from Eqs 31-35 that for  $n_p \gg n_f$ , the stagnant water in the micropores is the main reservoir for the tracer transport in fissured rocks. A serious error can be committed if that fact is not taken into account in the interpretation of water volume from the tracer age. In other words, stagnant water in the micropores, which is not available for exploitation, is the main contributor to the tracer age and the transport of pollutants.

## 10. Case studies

A number of case studies were reviewed in several papers [3, 6, 51]. Examples given below are selected to help the reader in a better understanding of different problems in practical applications of the lumped-parameter approach to different systems. In all these case studies, long records of tracer data were available. Unfortunately, very often single determinations of tritium, or another, tracer is available. Then, except for a constant tracer input, no age determination is possible. For springs with a constant outflow, two tritium determinations taken in a large time span are often sufficient to estimate the age. If for a given system a number of determinations are available with a short time span (up to about two years), a good practice is to "fit" the models which yield extreme age values (PFM and EM) for each sampling site and to take the mean value.

### 10.1. Granular aquifers

#### (a) *Ruszczka aquifer (Nowa Huta near Cracow, southern Poland)*

A sandy aquifer in Ruszczka is exploited by a number of wells (Figs 9 and 10). Its environmental tracer study was performed in order to compare different tracer techniques and to clarify if there is a flow component of a distant recharge [52]. On the basis of pumping tests it was supposed that all the wells are able to yield 10,000 m<sup>3</sup>/d for the recharge area limited by the boundary of the high terrace of Vistula (see Fig. 9). However, a long exploitation of all wells showed that it was possible to get only 6,000 m<sup>3</sup>/d, which still was too much for the supposed recharge area. On the other hand, high tritium and <sup>14</sup>C contents (76-71 pmc for  $\delta^{13}\text{C} = -15.3$  to  $-17.5$  ‰ [6, 33]) excluded the possibility of an underground recharge by older water.

Consider first the tritium interpretation reported in [25]. A number of dispersion models (DM) yielded equally good fits for the values of parameters listed in Table 1. It is evident that the  $\alpha$  coefficient cannot be used as a fitting parameter because then a large number of models (i.e., a large number of  $t_t$  and  $Pe$  pairs). The  $\alpha$  coefficient equal to about 0.60 was

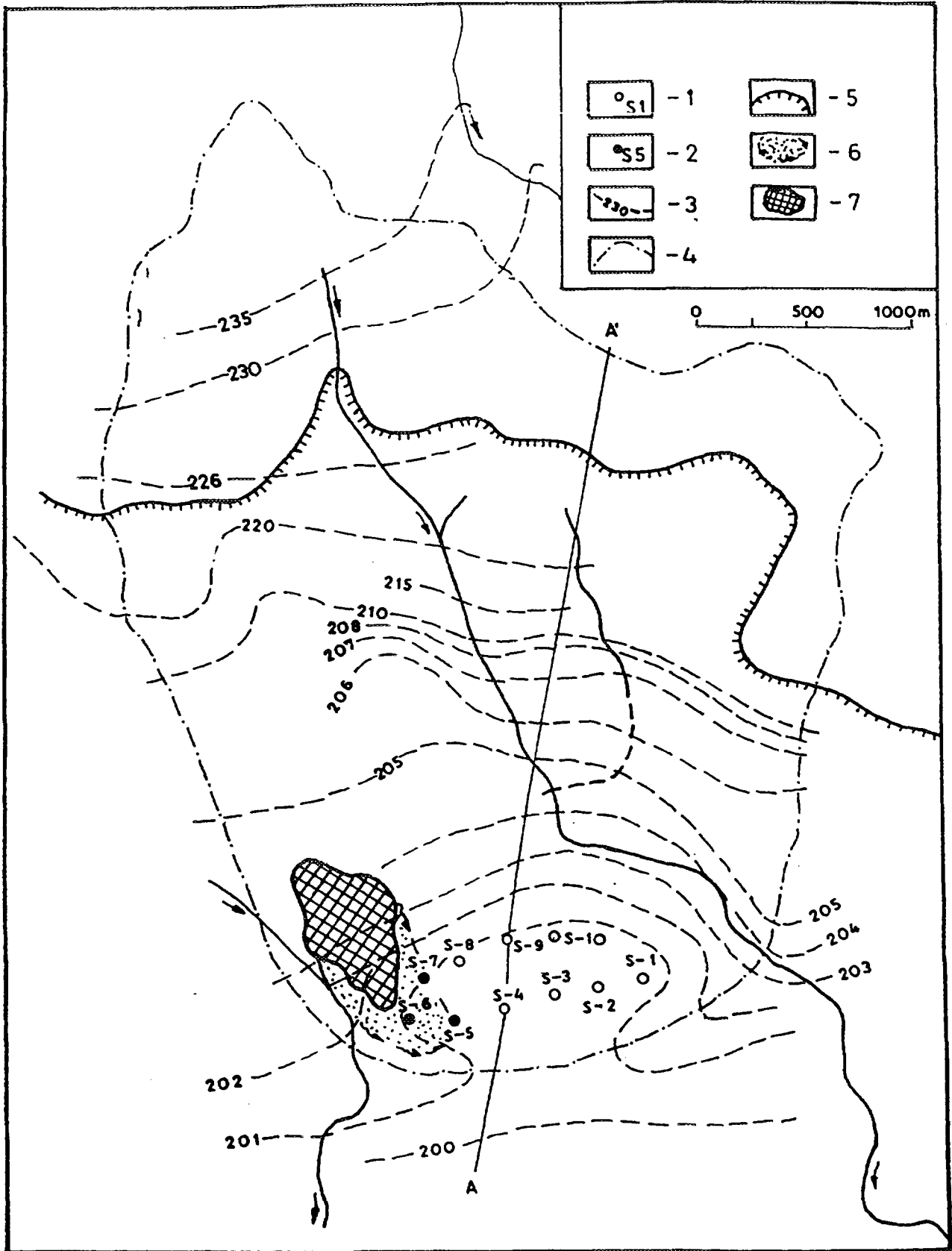


Fig. 9. Map of Ruszcza aquifer [52]. 1 - exploited wells, 2 - contaminated wells pumped as a barrier, 3 - piezometric surface, 4 - boundary of the recharge area defined by the flow lines and by the morphology in the northern part, 5 - boundary of the upper terrace of the Vistula river, 6 - contaminated part of the aquifer, 7 - disposal site.

Table 1. Tritium ages ( $t_t$ ) and the dispersion parameters ( $Pe^{-1}$ ) obtained from fitting the dispersion model (DM) to tritium data of Ruszcza wells for several  $\alpha$  values [25].

Well	$\alpha$	$t_t$ [a]	$Pe^{-1}$
S4	1.00	39.4	0.25
	0.77	38.4	0.25
	0.50	37.2	0.25
	0.40	36.8	0.25
	0.00	25.8	0.15
S1	1.00	30.6	0.15
	0.77	30.0	0.15
	0.50	29.4	0.15
	0.40	27.8	0.13
	0.00	21.3	0.08

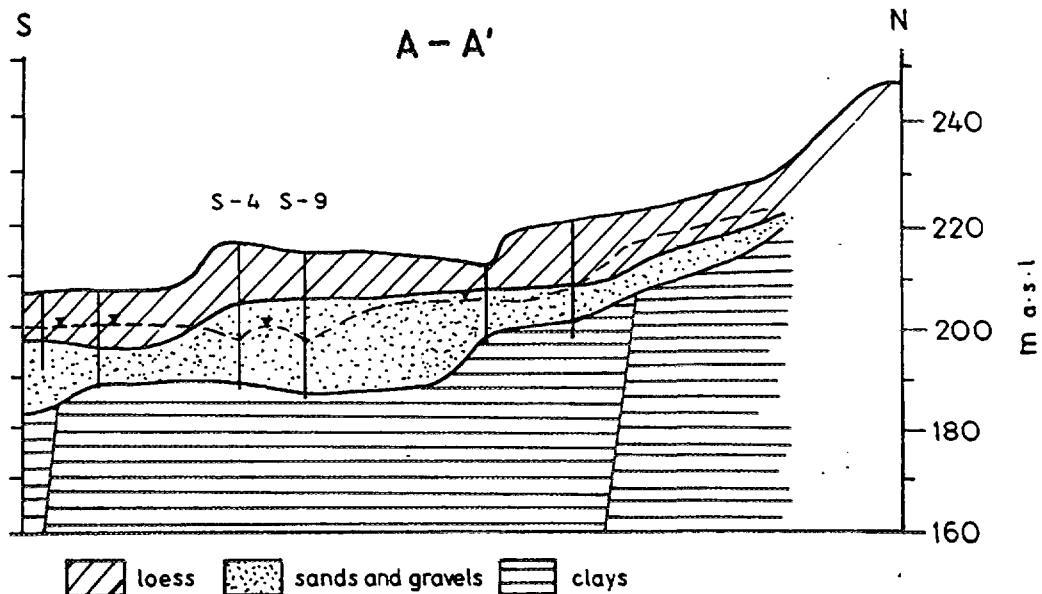


Fig. 10. Geological cross-section of Ruszcza aquifer [52].

found from Eq. 24 [for  $C_{in}$  replaced by  $\delta^{18}O$  (or  $\delta D$ ) of groundwater, and for summer and winter  $\delta^{18}O$  (or  $\delta D$ ) values calculated from mean monthly deltas and precipitation rates measured in Cracow station]. However, calculations performed for several assumed values of  $\alpha$  show that if  $\alpha \geq 0.4$ , its value does not influence strongly the value of age found from fitting (similar conclusion was reached for the Czatkowice study described further). Though the aquifer is unconfined, a relatively low value of the dispersion parameter qualitatively confirms the inadequacy of EM. On the other hand, due to a large reservoir in the unsaturated zone and its variable thickness, the dispersion model should be adequate.

Taking the mean tritium age of 35 years as equal to the mean water age, the following volume of water (V) in the system is obtained:

$$V = Qt_t = 6000 \text{ m}^3/\text{d} \times 35 \text{ years} \times 365 = 76.7 \times 10^6 \text{ m}^3 \quad (25)$$

The mean thickness of water is  $H_w = V/S_a = 7.1 \text{ m}$ , where  $S_a = 10.8 \times 10^6 \text{ m}^2$  is the surface of the recharge area defined by the morphology in the northern part and by the flow lines which reach the wells. The mean water thickness in the unsaturated zone ( $H_{wl}$ ) is in approximation given as the product of the loess layer thickness (12 m) and the mean moisture content by volume (0.32), i.e., about 3.8 m. From that the mean water thickness in the aquifer ( $H_{wa}$ ) is:

$$H_{wa} = H_w - H_{wl} = 7.1 - 3.8 = 3.3 \text{ m} \quad (26)$$

The mean age is also the sum of ages in the unsaturated ( $t_{t1}$ ) and saturated zones ( $t_{ta}$ ):

$$t_t = t_{t1} + t_{ta} \quad (27)$$

For the infiltration rate (I) estimated at about 0.20 m/year, the mean transit time through the unsaturated zone is:  $t_{t1} = H_{wl}/I = 3.8/0.2 = 19$  years. Therefore, the mean transit time through the saturated zone is from Eq. 27 equal to  $35 - 19 = 16$  years.

It is evident that the mean transit time of sulphates from the disposal site shown in Fig. 9, which was 23 years to the well S6 and 20 years to the well S7, practically resulted from the long transport in the unsaturated zone because the transit time in the saturated zone must be quite short due to a short distance and a large hydraulic gradient.

The mean water velocity ( $v_w$ ) for a porous aquifer can be estimated as follows:

$$v_w = (l/2)/t_{ta} = 100 \text{ m/year}$$

where  $l/2$  is a rough estimate of the mean flow length path ( $l$  being the length of the aquifer).

For the mean  $k$  value known from pumping tests ( $6 \times 10^{-4} \text{ ms}^{-1}$ ), the mean hydraulic gradient of 0.003 and the assumed porosity of 0.35, the water velocity is about 160 m/year, which reasonably agrees with the value estimated from the tracer data. For the total recharge area shown in Fig. 9, i.e., including the loess hills, the available flow rate is:  $Q = I \times S_a \approx 6000 \text{ m}^3/\text{d}$ .

It should be mentioned that the model obtained from the tritium data yielded a reasonable agreement also for the  $^{14}\text{C}$  data [6, 32] whereas no fit was obtained for the  $^3\text{H-He}^3$  and  $^{85}\text{Kr}$  methods [32]. In the case of the  $^3\text{H-He}^3$  method, the observed  $\text{He}^3$  concentrations were lower than expected from the prediction obtained with the aid of the tritium model. The escape of  $\text{He}^3$  by diffusion from its peak in the unsaturated zone, which is related to the bomb peak of  $^3\text{H}$  can be offered as an explanation. On the other hand,  $^{85}\text{Kr}$  concentration were about three times higher than predicted values. In that case, a faster diffusion transport of  $^{85}\text{Kr}$  from the atmosphere to the aquifer, in comparison with the velocity resulting from the infiltration rate through the unsaturated zone, can be offered as a possible source of the discrepancy. A similar picture was observed for freon-11. Therefore, it was

concluded that the tritium method yielded reasonable results whereas the  $^3\text{H-He}^3$ ,  $^{85}\text{Kr}$  and freon-11 methods failed. Even if these methods are improved in near future, their accuracy will probably be lower than the present accuracy of the tritium method.

(b) *An alpine basin, Wimbachtal Valley, Berchtesgaden Alps, Germany*

The Wimbachtal Valley has a catchment area of  $33.4 \text{ km}^2$ , and its groundwater system consists of three aquifer types with a dominant porous aquifer. The environmental isotope study was performed to provide a better insight into the groundwater storage properties [41]. Due to lack of other possibilities, the system was treated as a single box. The direct runoff is very low and for the period of observations its mean value was estimated to be less than 5 %. However, the presence of direct runoff as well as changes in flow rate and volume contribute to a large scatter of tracer data.

In five river sampling points the tritium output concentrations were measured for 3.5 years and  $\delta^{18}\text{O}$  values for 3 years. A very favourable situation because the input data were available from a station situated in the valley. The results of fittings for the river sampling points are summarized in Table 2.

Table 2. Mean transit times ( $t_t$ , in years) for EM, and for DM with two values of the dispersion parameters ( $\text{Pe}^{-1}$ ), obtained for tritium and  $\delta^{18}\text{O}$  (in brackets), after [41] with minor corrections.

Sampling point	EM	DM ( $\text{Pe}^{-1} = 0.12$ )	DM ( $\text{Pe}^{-1} = 0.6$ )
River, A	4.8	7.0	4.2 (4.1)
B	3.9	6.2	3.8
E	4.1 (4.0)	6.4 (n.o.)	4.0 (4.0)
F	3.9	6.2	3.7 (3.8)
P	4.3 (4.5)	6.5 (n.o.)	4.2 (4.1)

n.o. - a "good fit" was not obtainable.

It is evident from Table 2 that in spite of large number of tritium data no unambiguous calibration of DM was obtained due to a large scatter of tritium contents. Due to a complex hydrogeology of the system, the higher value of the dispersion parameter seems to be more probable, especially as no good fit was obtained for the lower dispersion parameter in the case of oxygen-18 (see Table 2). A good fit obtained for EM also indicates that the dispersion parameter of 0.12 is unacceptable.

For the mean tracer age of 4.15 years, and the mean discharge of  $1.75 \text{ m}^3 \text{ s}^{-1}$  (in the period 1988-1991), the water volume of  $230 \times 10^6 \text{ m}^3$  was obtained. However, the mean water volume estimated from the rock volume and the porosity (with a correction for the unsaturated zone) is  $470 \times 10^6 \text{ m}^3$ , i.e. about two times more than the volume found from the tracer method. saturated yields the water volume of  $600 \times 10^6 \text{ m}^3$ . No plausible explanation for this discrepancy was given in the original work. A possible existence of large stagnant zones, i.e., sedimentation pockets or deep layers separated by semi-permeable interbeddings from the upper active flow zone, to which the diffusion and advection of tracer are negligible can be offered as an explanation of that discrepancy (see Sect. 9.2).

It should be mentioned that the  $\alpha$  coefficient estimated from Eq. 25 was equal to 0.17 (in the original work it was given in approximation as equal to 0.2) whereas a direct estimation from the precipitation and outflow rate data yielded about 1. That discrepancy can be explained by large storage of snow in winter months, which melts in summer months.

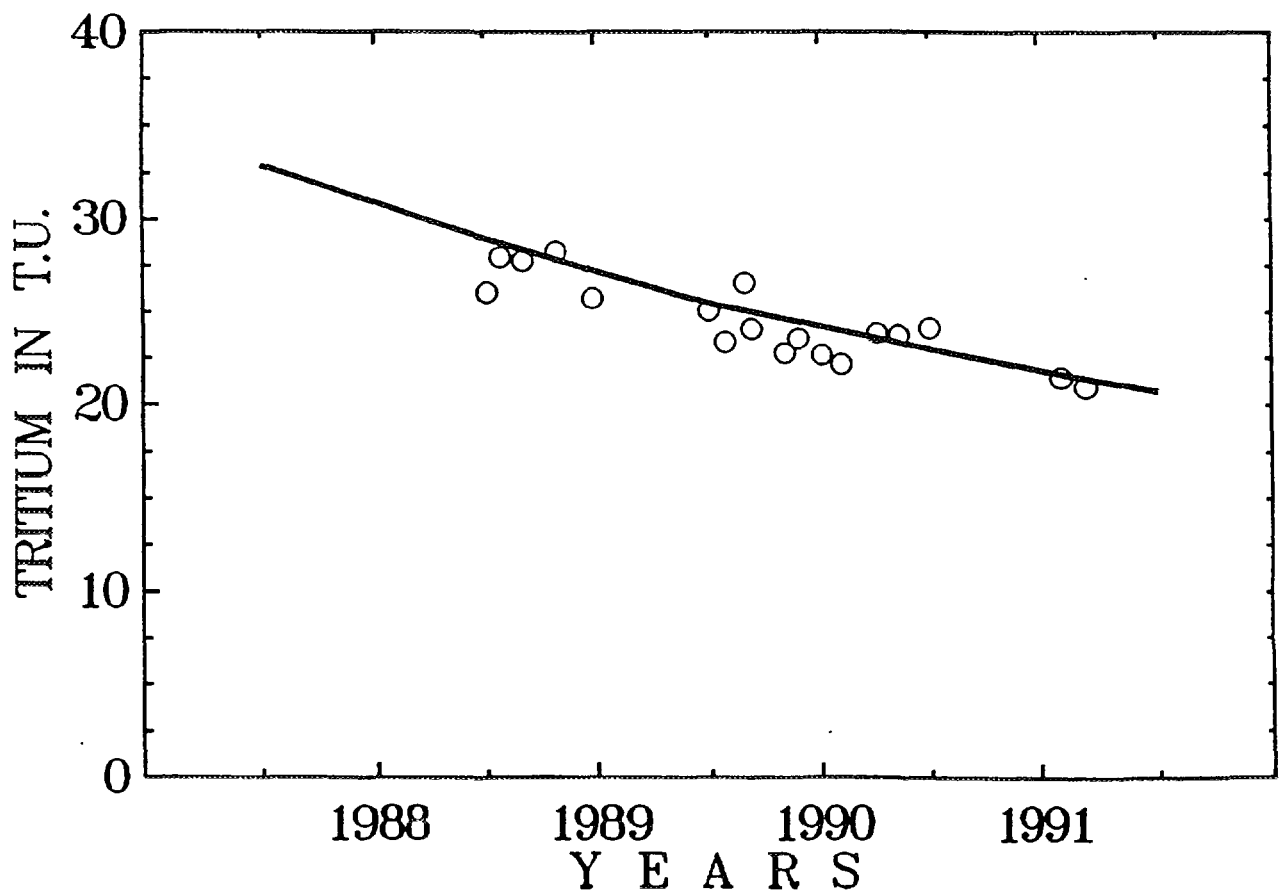
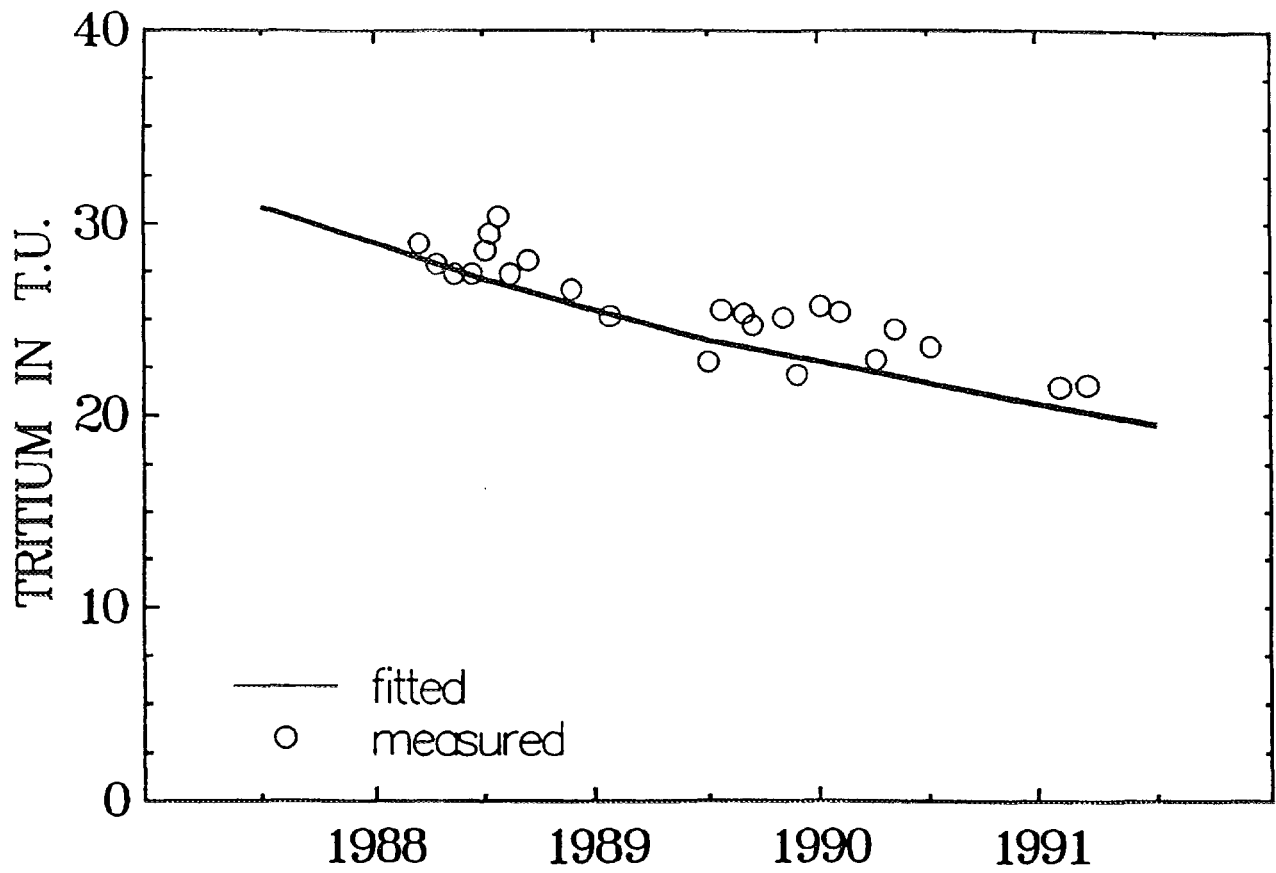


Fig. 11. Upper: Observed and fitted tritium output function for total runoff at Wimbach gauging station (A in Table 2). Lower: Observed and fitted tritium output function for Wimbachquelle (Wimbach spring, F in Table 2).

(c) *River bank infiltration, Passau, Germany*

In river bank infiltration studies the advantage is taken of the seasonal variations in the stable isotope composition of river water, and of the difference between its mean value and the mean value of groundwater. Measurements of  $\delta^{18}\text{O}$  were used to determine the fraction of bank infiltrated river water making up the groundwater of a small island ( $0.3 \text{ km}^2$ ) in the Danube River near Passau [54]. In Fig. 11 a schematic presentation of flow pattern and its lumped-parameter model is shown. The portion of the river water ( $p$ ) was calculated from the mean tracer contents applying the following formula:

$$p = \frac{\left[ \overline{\delta^{18}\text{O}}_x - \overline{\delta^{18}\text{O}}_{ow} \right]}{\left[ \overline{\delta^{18}\text{O}}_d - \overline{\delta^{18}\text{O}}_{ow} \right]} \quad (28)$$

where subscripts are as follows:  $x$  is for the wells on the island,  $d$  is for the Danube water, and  $ow$  is for the observation well (see Fig. 13).

Due to the seasonal variations of the Danube water, the water exploited in the island has also variable isotopic composition. The following formula was applied adequately to the situation shown in Fig. 13:

$$C(t) = p \int_0^{\infty} C_{in}(t - t')g(t')dt' + (1 - p)\overline{\delta^{18}\text{O}}_{ow} \quad (29)$$

where  $C_{in}(t)$  function was taken as the weighted monthly means of the delta values in Danube water. Due to very short mean transit times (48 to 120 d), it was possible to fit equally well three models, EM, EPM with  $\eta = 1.5$  and DM with  $Pe^{-1} = 0.12$ . Apparent dispersivities ( $D/v$ ) calculated for particular wells from the dispersion parameter varied between 2.3 m to 25 m as the result of long injection lines along the bank. For the identified input-output relation it was possible to predict response of the wells to hypothetical pollutant concentration in river water (DM was chosen for that purpose). A similar study was presented in [55] whereas in [56] a slightly more complicated case was described, which however was finally simplified to Eq. 29.

## 10.2. *Fractured rocks*

(a) *Czatkowice springs (Krzyszowice near Cracow, southern Poland)*

Czatkowice springs discharge water from a fissured and karstified carbonate formation at a crossing of two fault zones which act as impermeable walls [13]. The Nowe ( $60 \text{ ls}^{-1}$ ) and Wrobel ( $12 \text{ ls}^{-1}$ ) springs have the same tritium concentration (about 10 T.U.) which is nearly constant in time. The tritium content in the Chuderski spring ( $18 \text{ ls}^{-1}$ ) was about 45 T.U. in 1974, and decreased to about 18 T.U. in 1984. Similarly to the case study in Ruszcza, it was shown that when  $\alpha$  coefficient is included in the fitting procedure, no unambiguous solution can be obtained. The stable isotopes yielded  $\alpha = 0.63 \pm 0.13$  for  $\delta^{18}\text{O}$  and  $\alpha = 0.76 \pm 0.15$  for  $\delta\text{D}$ . For more recent fittings shown in Tables 3 and 4, and in Figs 12 and 13, the  $\alpha$  coefficient was assumed to be equal to 0.77. Initially, according to [24], it was not possible to obtain good fits for the Nowe and Chuderski springs without assuming the presence of an old water component without tritium. In a recent interpretation, which included additional tritium determinations, it was possible to obtain a good fit for the Nowe spring without an old component (see Table 3) whereas for the Chuderski spring two versions of the old component were considered (see Table 4 and Fig. 13). However, it is evident that in spite of a long tritium record of about 10 years, no unambiguous fitting was possible. The results given for the Nowe and Wrobel springs suggest the EPM to be the

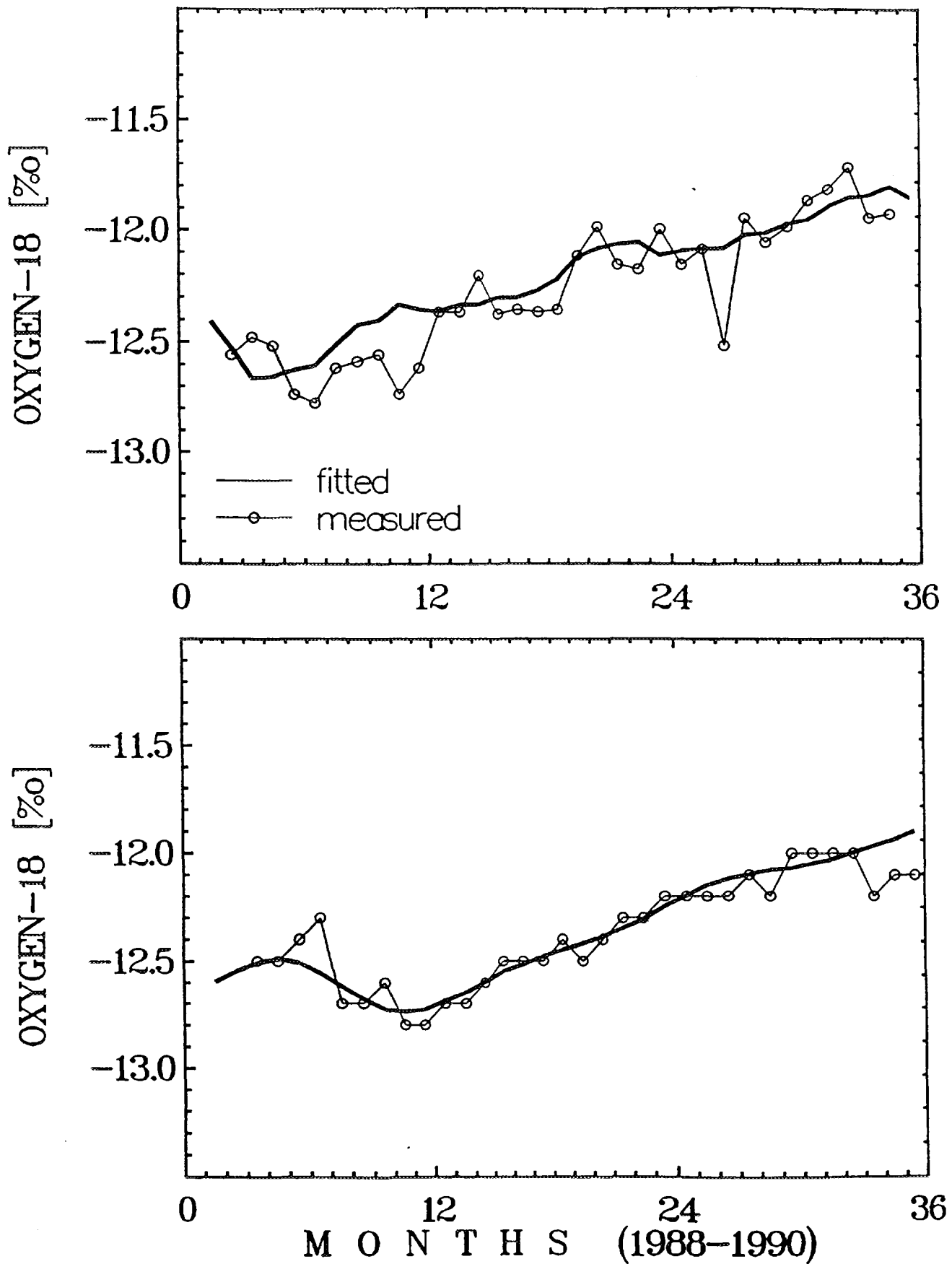


Fig. 12. Upper: Observed and fitted  $^{18}\text{O}$  output function for total runoff at Wimbach gauging station (A in Table 2). Lower: Observed and fitted  $^{18}\text{O}$  output function for Wimbachquelle (Wimbach spring, F in Table 2).



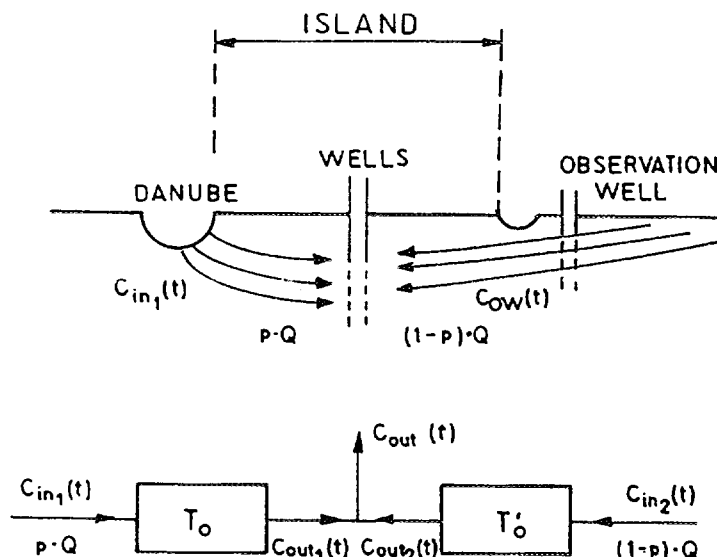


Fig. 13. Conceptual model of river bank filtration in Passau (notation as in the original paper [54]):  $p$  - represents the fraction of river water and  $1 - p$  is the fraction of local groundwater. Note that  $1 - p$  is equivalent to  $\beta$  defined in Sect. 4.1 and applied in the FLOW program (Appendix C).

most reliable, because for that model a relatively good fit is obtained for two parameters, whereas in other cases either the number of parameters is larger or the accuracy lower. In other words, it is possible to obtain a reasonable fit without assuming the presence of a tritium free component, but the tritium age is quite high (note that the mean age can be much larger than the time span since the beginning of hydrogen bomb tests, which is the consequence of the wide spectrum of the transit times for given response functions).

Table 3. Models fitted to the Nowe spring tritium data [7].

Number	Model	$t_t$ [a]	$Pe^{-1}$	$\eta$	$\beta$	$\sigma$ [T.U.]
For 0 T.U. in old component						
1	DM	130	1.0	-	0.70	0.546
2	DM	70	0.5	-	0.78	0.510
3	DM	95	0.5	-	0.58	0.475
Without old component						
4	DM	190	0.8	-	-	0.622
5	DM	135	0.5	-	-	0.736
6	EM	400	-	(1.00)	-	0.906
7	EPM	300	-	1.04	-	0.522

For the Chuderski spring also a number of models can be fitted, especially as two flow components seem to exist. In the early interpretation, similarly to the Nowe and Wrobel springs, it was assumed that the older component is tritium free [24]. That assumption is represented by models 1, 2, and 3 in Table 4 and Fig. 13. However, if EPM (No 7 in Table 2, i.e., a

model without an old component) is chosen for the Nowe and Wrobel springs, which are situated just at lower elevation than, and close to the Chuderski spring, it is more reasonable to assume that the old component in that spring is exactly the same as water discharged from the other two springs. In such a case, in a good approximation, the tritium content of 10.7 T.U. in the old component can be taken as the mean value for the period of observations. Then, the models No 5-8 in Table 4 and Fig. 13 are obtained. Model No 8 can be selected as that with the lowest number of fitting parameters and the best fit. In conclusion 15 % of water in the Chuderski spring is young and recharged at a local hill, whereas 85 % and 100 % of the Nowe and Wrobel springs come from a larger distance. The whole aquifer is unconfined, but paleo-channels close to the Nowe and Wrobel springs act as a piston flow model of a low volume (about 4 % of the total volume because  $\eta = 1.04$ ).

Table 4. Models fitted to the Chuderski spring tritium data [7].

Number	Model	$t_t$ [a]	$Pe^{-1}$	$\beta$	$\sigma$ [T.U.]
For 0 T.U. in old component					
1	DM	15	0.25	0.82	0.815
2	DM	20	0.25	0.78	0.766
3	DM	30	1.0	0.73	0.922
-----					
For 10.7 T.U. in old component					
5	DM	12	0.8	0.85	0.837
6	DM	3	0.9	0.75	1.059
7	EM	2.5	-	0.75	1.067
8	EM	11	-	0.85	0.757

Details of the hydrogeological interpretation can be found in [13]. Here, only the most important findings are given. For the mean matrix porosity of  $0.030 \pm 0.005$  (known from laboratory measurements on core samples), the mean distance between the centre of the recharge area and springs of  $8000 \pm 2000$  m, and the mean hydraulic gradient of  $0.006 \pm 0.001$  (both known from the hydrogeological map), Eq. 33 yields  $k = (4.2 \pm 1.5) \times 10^{-6} \text{ ms}^{-1}$ , which agrees well with other estimates. Similarly, the local hydraulic conductivity found from the age of the young component in the Chuderski spring agrees reasonable with other estimates.

The fissure porosity of 0.0015 is known from direct observation in a nearby quarry. If the tritium age is wrongly identified with the water age in a simplified form of Darcy's law, it yields  $k = n_f x / [t_t (\Delta H / \Delta x)] = 0.2 \times 10^{-6} \text{ ms}^{-1}$ , which is about 20 times too low.

It should be mentioned that for the Nowe and Chuderski spring, preliminary  $^{85}\text{Kr}$  and  $^3\text{He}$  measurements did not agree with the expected values found for the models fitted to the tritium data [32]. No reinterpretation has been performed so far for the new approach to the tritium data, which is presented here after [7].

*(b) Thermal systems in Cieplice and Ladek Spas, Sudetes, Poland*

The main granitic thermal system in Cieplice Spa contains water which according to stable isotope composition,  $^{14}\text{C}$  content and noble gas data can be dated to the end of the last glacial period [57]. The  $^{14}\text{C}$  age was estimated by the piston flow approach for a steady tracer input, whereas the shift in the stable isotope content caused by climatic change can be consid-

ered as a transient state tracer input. Water volume was found from Eq. 34, and for known matrix porosity (about 0.02), the rock volume was given by Eq. 35. That rock volume was shown to reasonably agree with the estimate based on the morphology of the basin and the depth of aquifer, whereas any estimate for a neglected matrix porosity would lead to an unacceptably high rock volume. The simplified form of Eq. 33 yielded a reasonable value of the hydraulic conductivity, which also confirmed the importance of matrix porosity as a transport parameter.

The thermal water in Ladek Spa, which discharges from gneisses of low matrix porosity (about 0.008) was shown to have the PFM-<sup>14</sup>C age of several thousand years [58]. In spite of low matrix porosity, also in that system Eqs 33-35 were shown to be applicable and yield reasonable results whereas any identification of tracer ages with the mobile water in fissures would yield unacceptable results.

(c) Cheju Island, South Korea

First isotopic investigations performed on Cheju Island were described in [59] where a binomial model was used to interpret the tritium data. The same data were later interpreted with the aid of EM and EPM which yielded much better fits than those obtained in the original paper [3, 6]. For a large coastal spring (site 2), EM yielded age of 19 years whereas EPM gave 21 years with  $\eta = 1.1$ . However, the stable isotope composition showed that the spring has its recharge area at high altitude, at the central part of the island, excluding the possibility of a significant recharge at the large coastal plain. Therefore, EM can be rejected, and  $\eta = 1.1$  means that the main water body with an exponential flow pattern is probably in the mountains whereas from there water is led to the coast by a small volume system (a lava tunnel?). This example shows how stable isotope data can be used in a qualitative way to identify a more adequate model. Unfortunately, no data are available on the relation between mobile and immobile water volumes. However, the tritium ages are most probably related to a high degree to the stagnant water in a microporous lava.

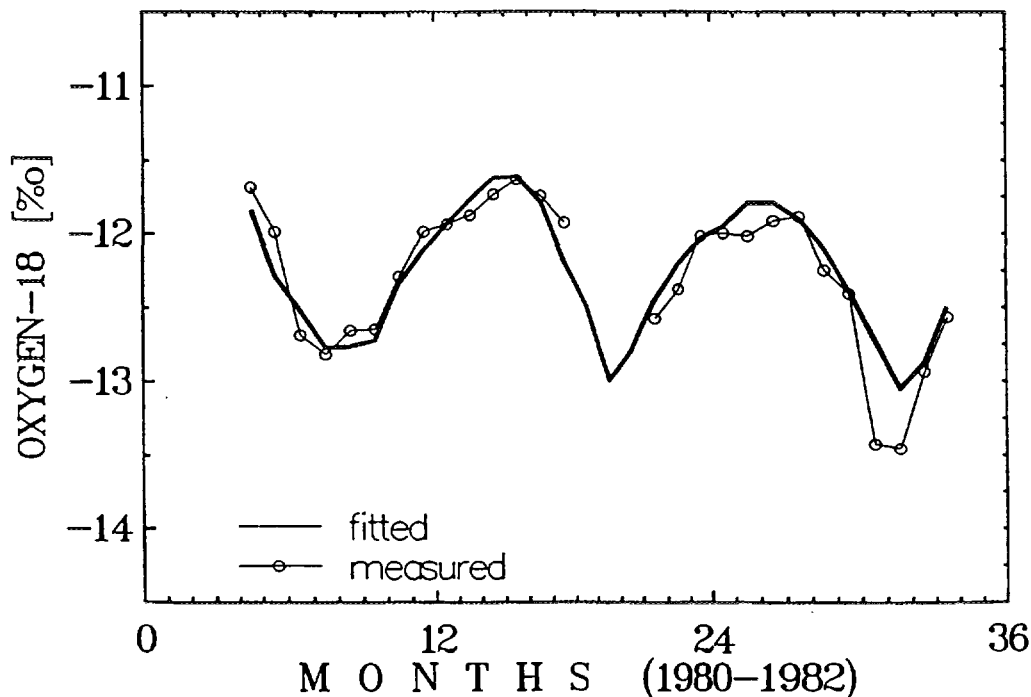


Fig. 14. Observed and fitted <sup>18</sup>O output function in PSI well in Passau for DM with  $t_t = 60$  days,  $D/vx = 0.12$ ,  $1 - p = \beta = 0.80$ ,  $C_\beta = -10.4$  ‰ [54].

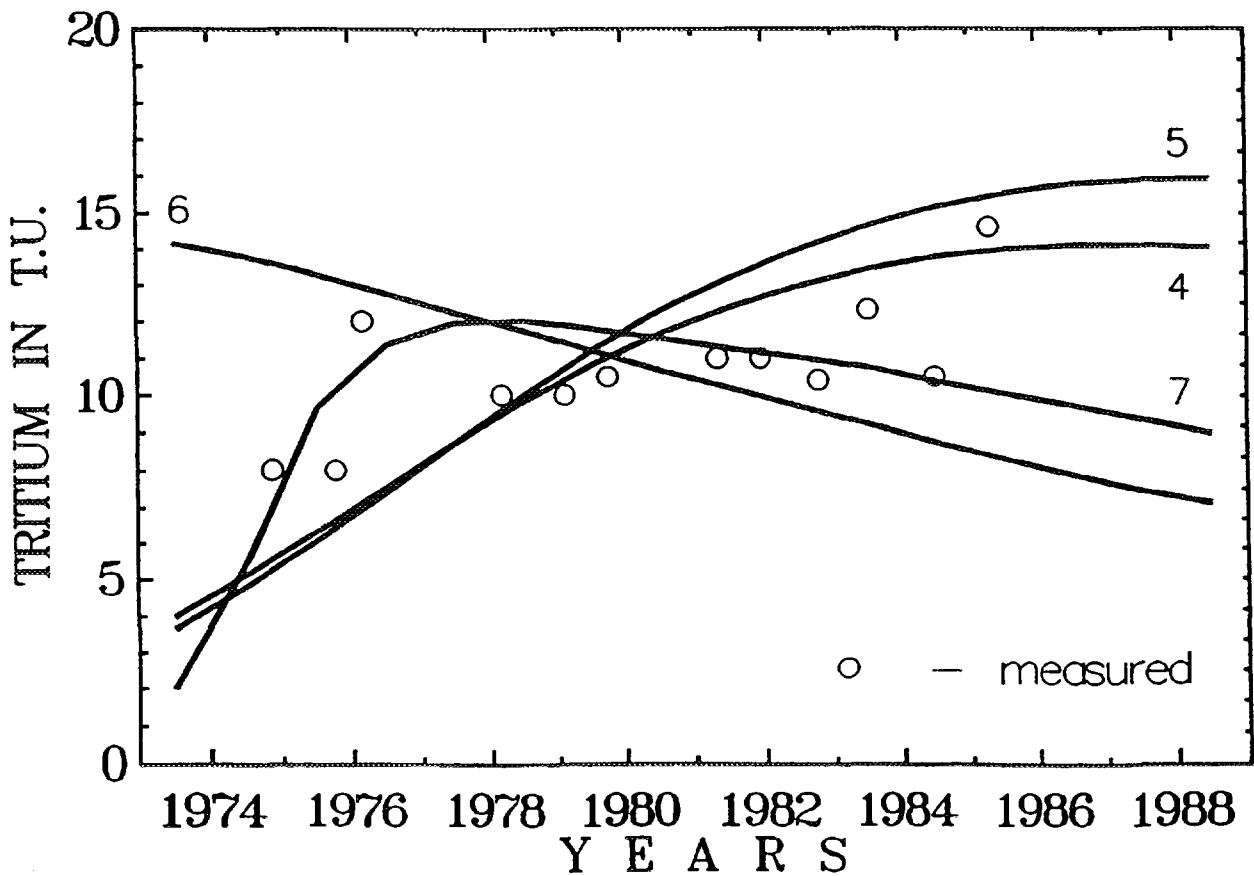
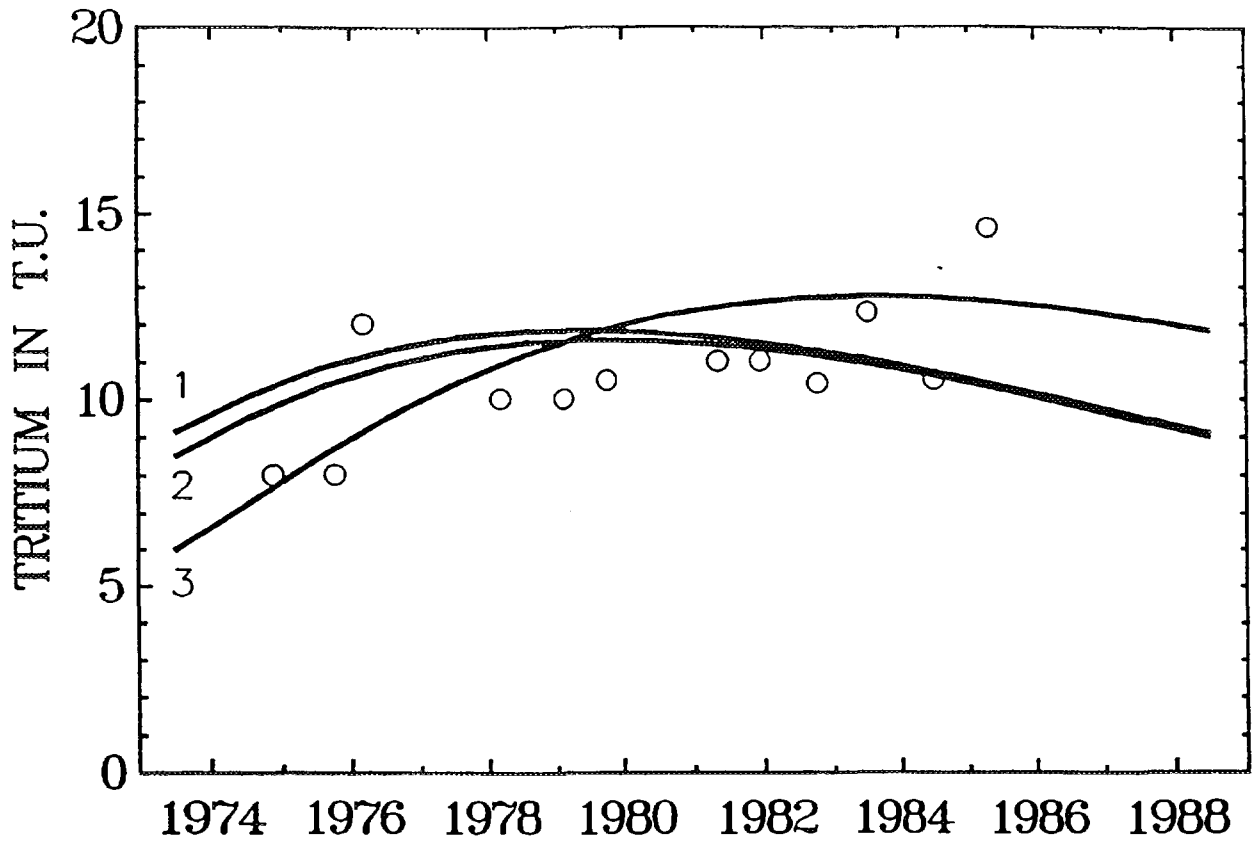


Fig. 15. Different models fitted to the tritium data of the Nowe spring (curve numbers correspond to model numbers in Tab. 3) [7].

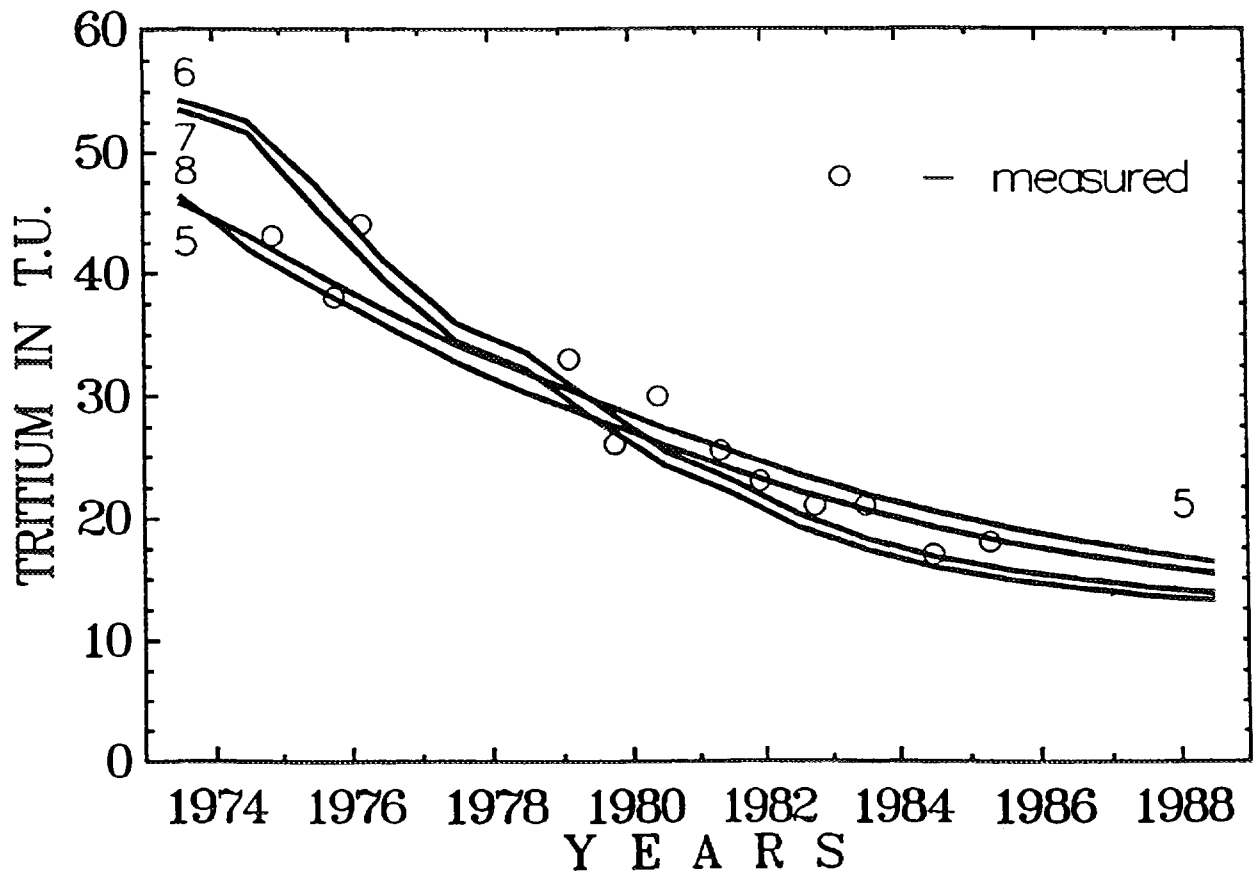
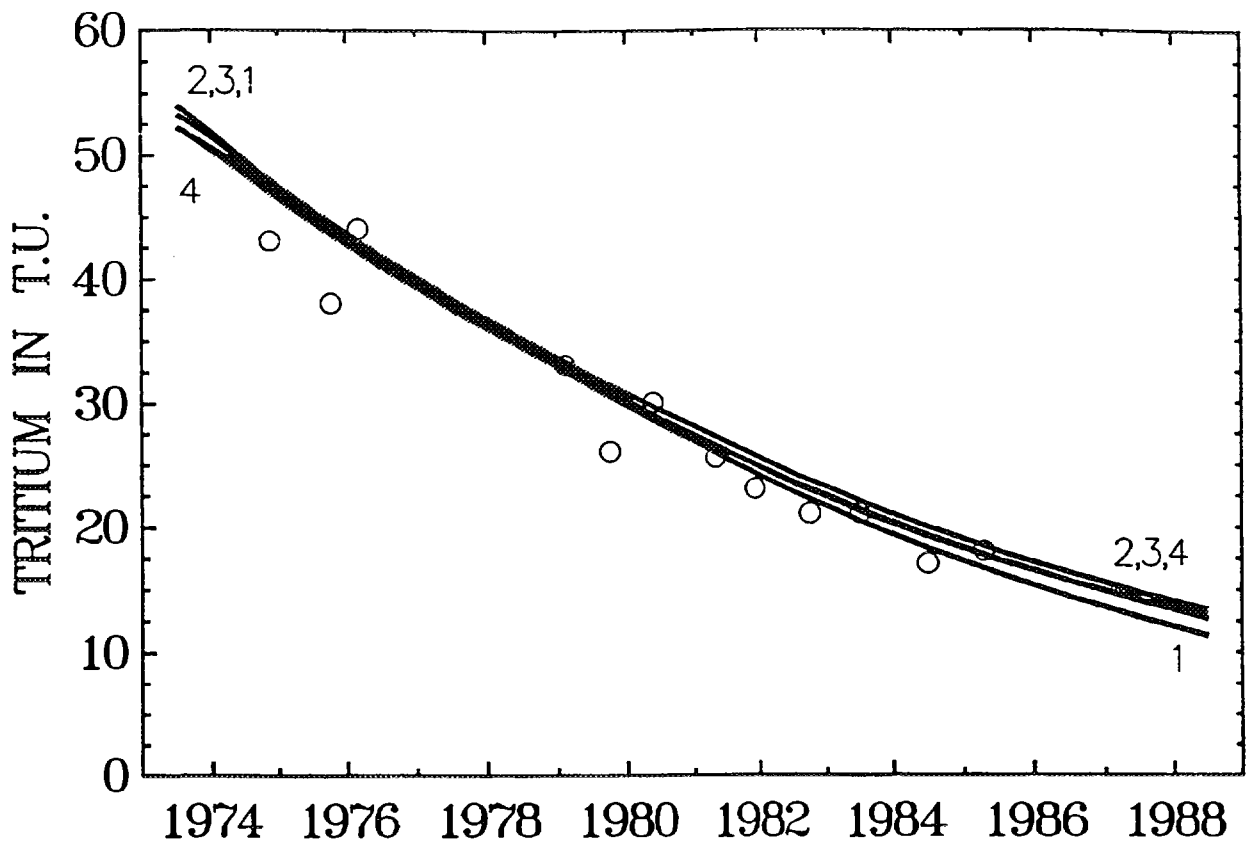


Fig. 16. Different models fitted to the tritium data of the Chuderski spring (curve numbers correspond to model numbers in Tab. 4) [7].

### 10.3. Complex cases

#### (a) An alpine basin, Lainbach valley, Germany

A complex interpretation was described for an alpine basin with a catchment area of  $18.7 \text{ km}^2$  [60]. Three conceptual models shown in Fig. 14 were considered. First, the direct runoff was eliminated. Another trick to solve a complex problem was to use seasonal variations in deuterium content to find the transit time through the upper reservoir (the tracer is stable, and, therefore, its flow through a large deeper reservoir does not influence the shift of seasonal variations in response). Tritium samples were taken only for base flow and served to calculate the mean transit time both for model 2 and for model 3 (see Fig. 14). For details of the study, the reader is referred to the original paper.

#### (b) A small basin in Harz Mountains

A detailed study of a small basin ( $0.76 \text{ km}^2$ ), Lange Bramke, Harz Mts., Lower Saxonia, was first given in [61] and extended in [60]. The interpretation of tritium data for a single reservoir both for steady flow approximation and variable flow approach was given in [46] as mentioned in Sect. 8.

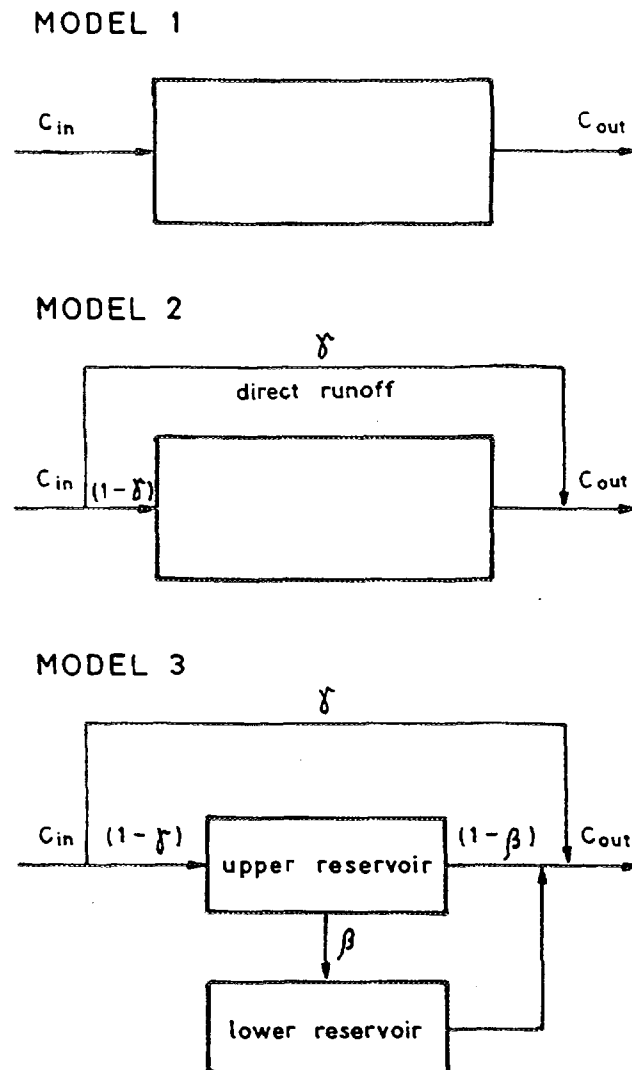


Fig. 17. Three scenarios of the Lainbach valley conceptual model [60].

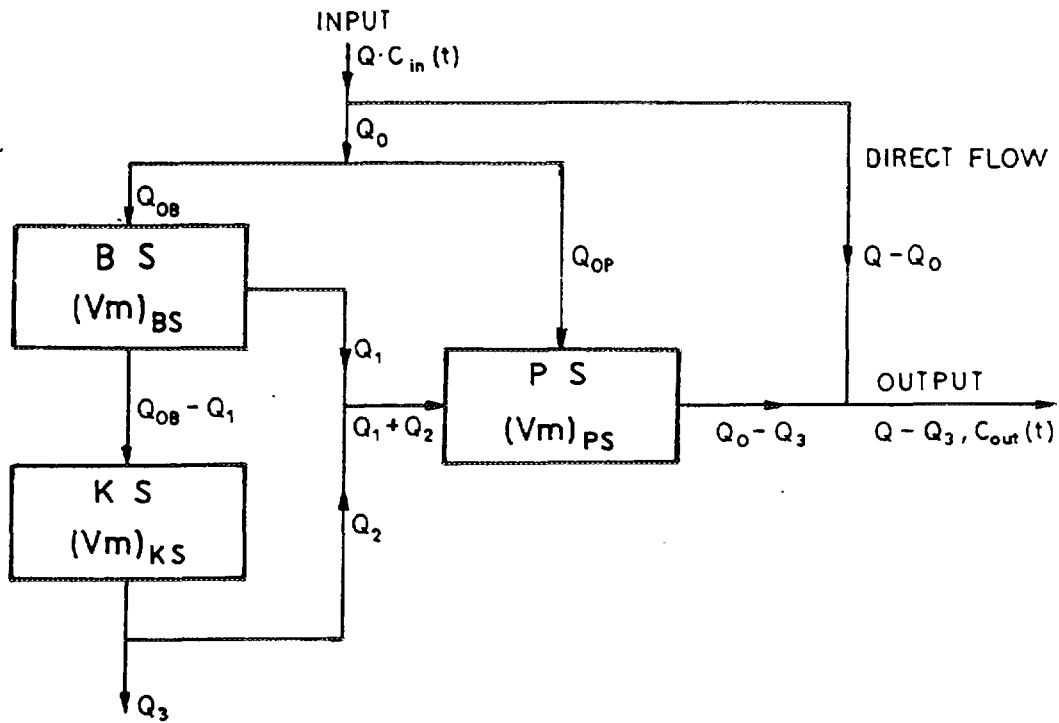


Fig. 18. Lange Bramke conceptual model [61, 62].

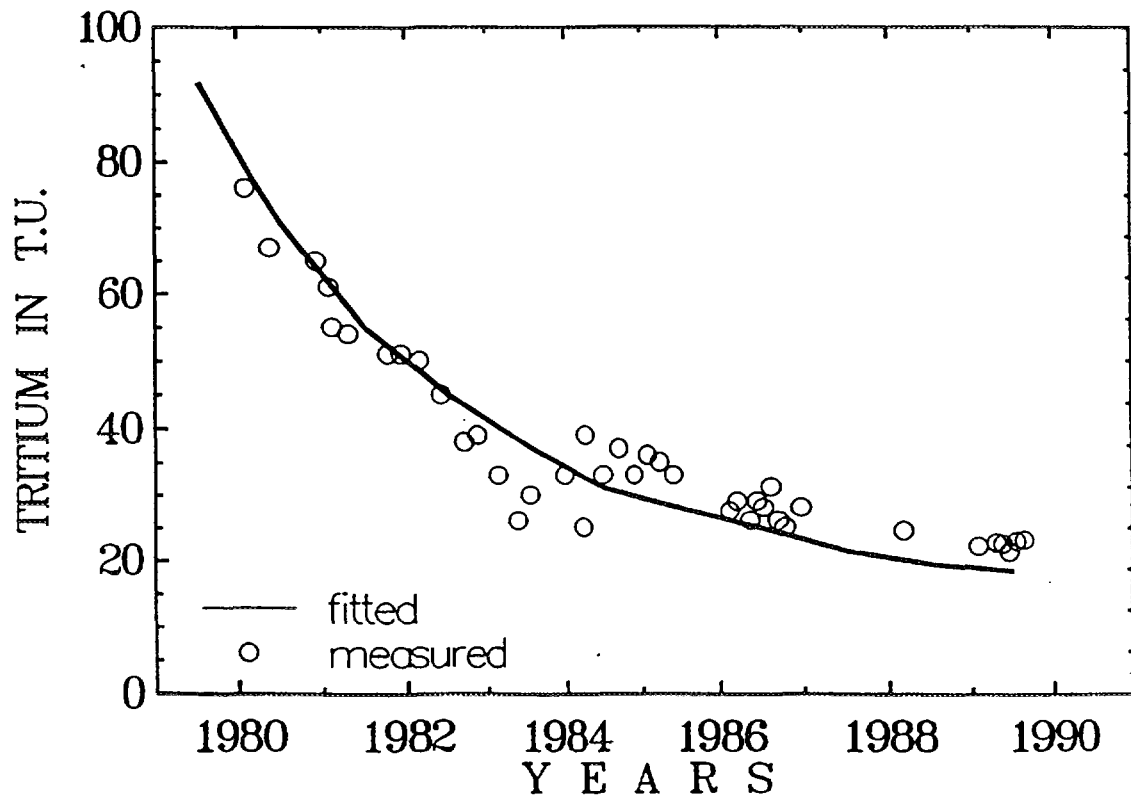


Fig. 19. Observed and fitted tritium output functions for the stream draining the Lange Bramke basin [61, 62].

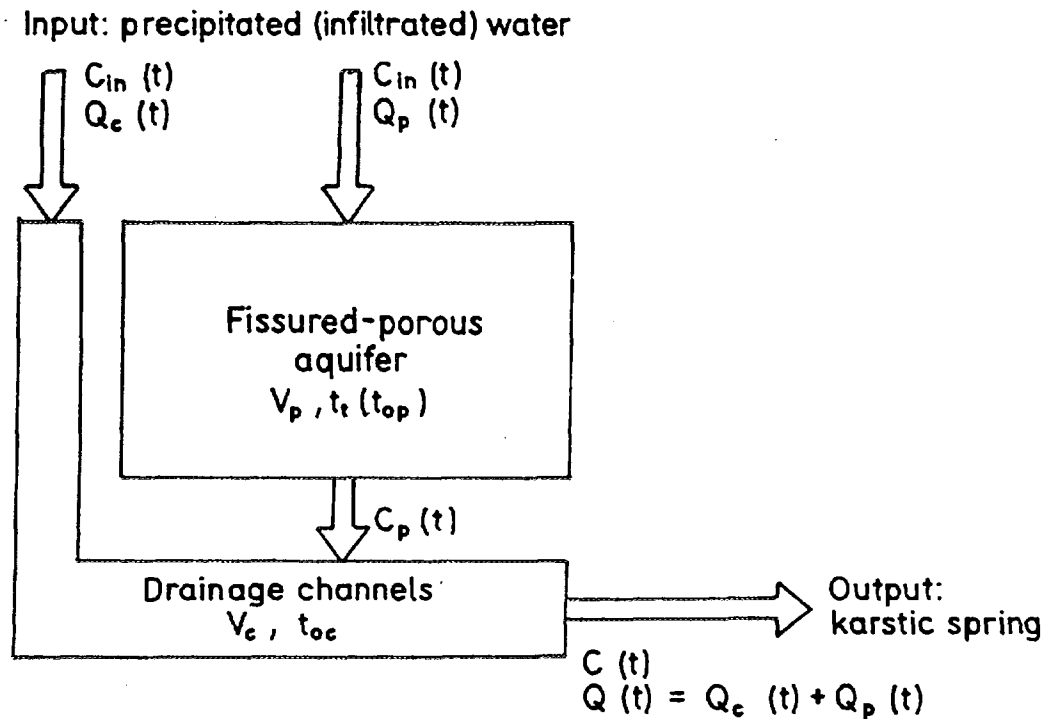


Fig. 20. Schneealpe massif conceptual model (notation as in the original paper [64]).

In Fig. 15 a more complex conceptual model is shown [62]. The BS box represents unsaturated zone associated with different soil materials which cover KS. The KS box represents fissured rock whereas the PS is for the porous reservoir located in the valley bottom. Tritium was measured at the outflow from the basin for low flow (in  $Q_0 - Q_3$  in Fig. 15). Oxygen-18 was measured in precipitation ( $Q$ ), direct flow ( $Q - Q_0$ ) and in total surface outflow ( $Q - Q_3$ ). The flux through the BS reservoir was measured by sampling for  $^{18}\text{O}$  at different depths whereas the flow in the PS was sampled for the same tracer with the aid of piezometers screened at required depths. However, in spite of considerable expenses, it was not possible to identify fully the whole system due to the lack of information on some flow components and on the fissured part (KS).

#### 10.4. Complex cases in karstic rocks

##### (a) General comments

Tracer data from karstic rocks, in which large channels collect water only at final stages, can often be interpreted similarly to fissured rocks, i.e. as if the movement were taking place in the total open porosity. This was shown for the Czatkowice springs discussed above. A similar conclusion was reached for a pollutant movement in a karstic-fissured-porous formation in which large karstic forms are developed in vertical direction, and are discontinuous in the direction of flow [63]. However, in karstic rocks, continuous channels extending from sinkholes in the recharge area to springs are often observed, and then the interpretation is difficult. An example of the interpretation of such a system by combination of two tracers is given below.



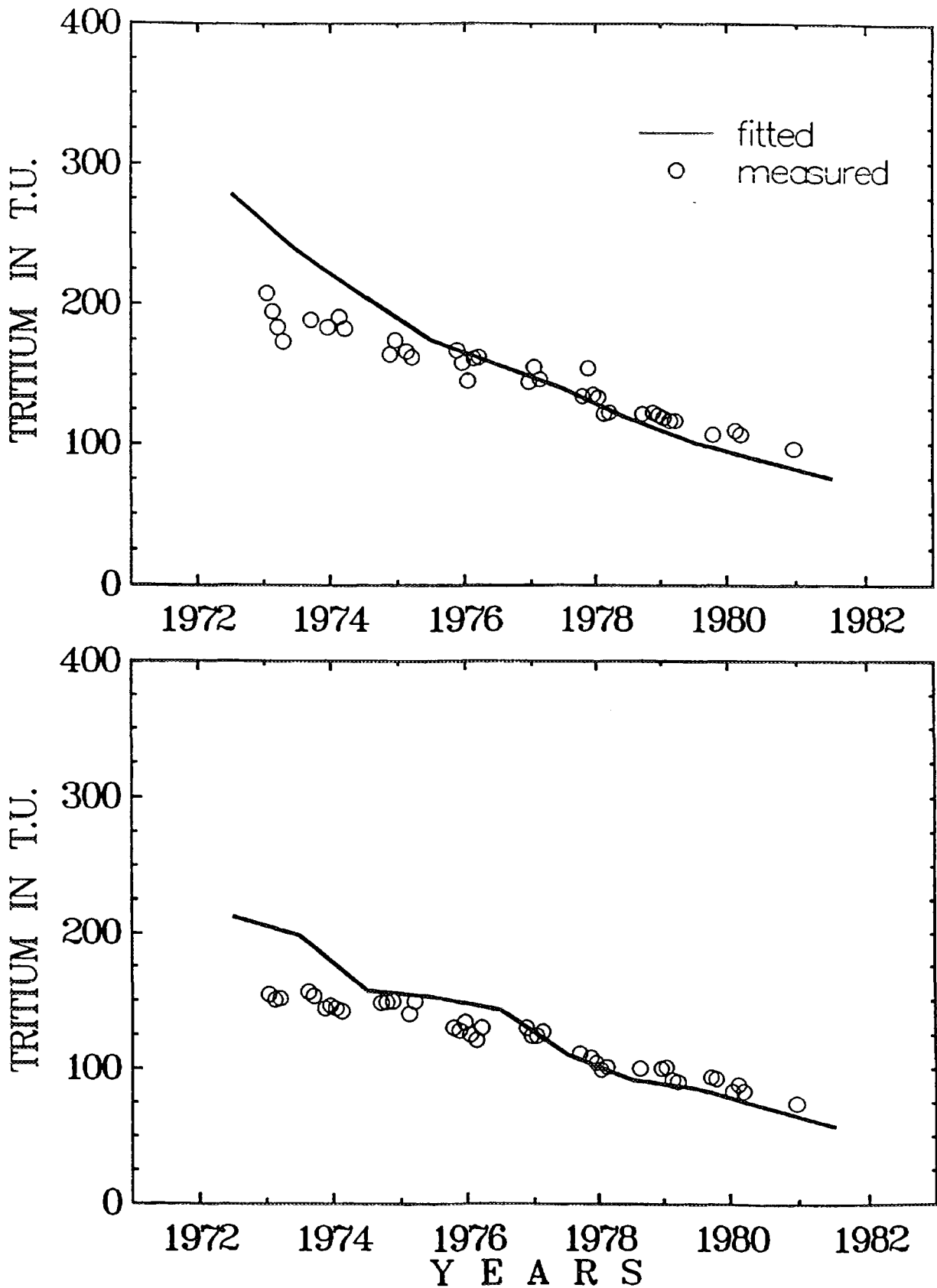


Fig. 21. Schneetalpe massif tritium output functions Wasseralquelle (upper) and Siebenquelle (lower) observed for base flow. Dispersion models (DM) with  $D/vx = 0.5$  and  $t_t$  of 4.5 and 2.5 years, respectively [64].

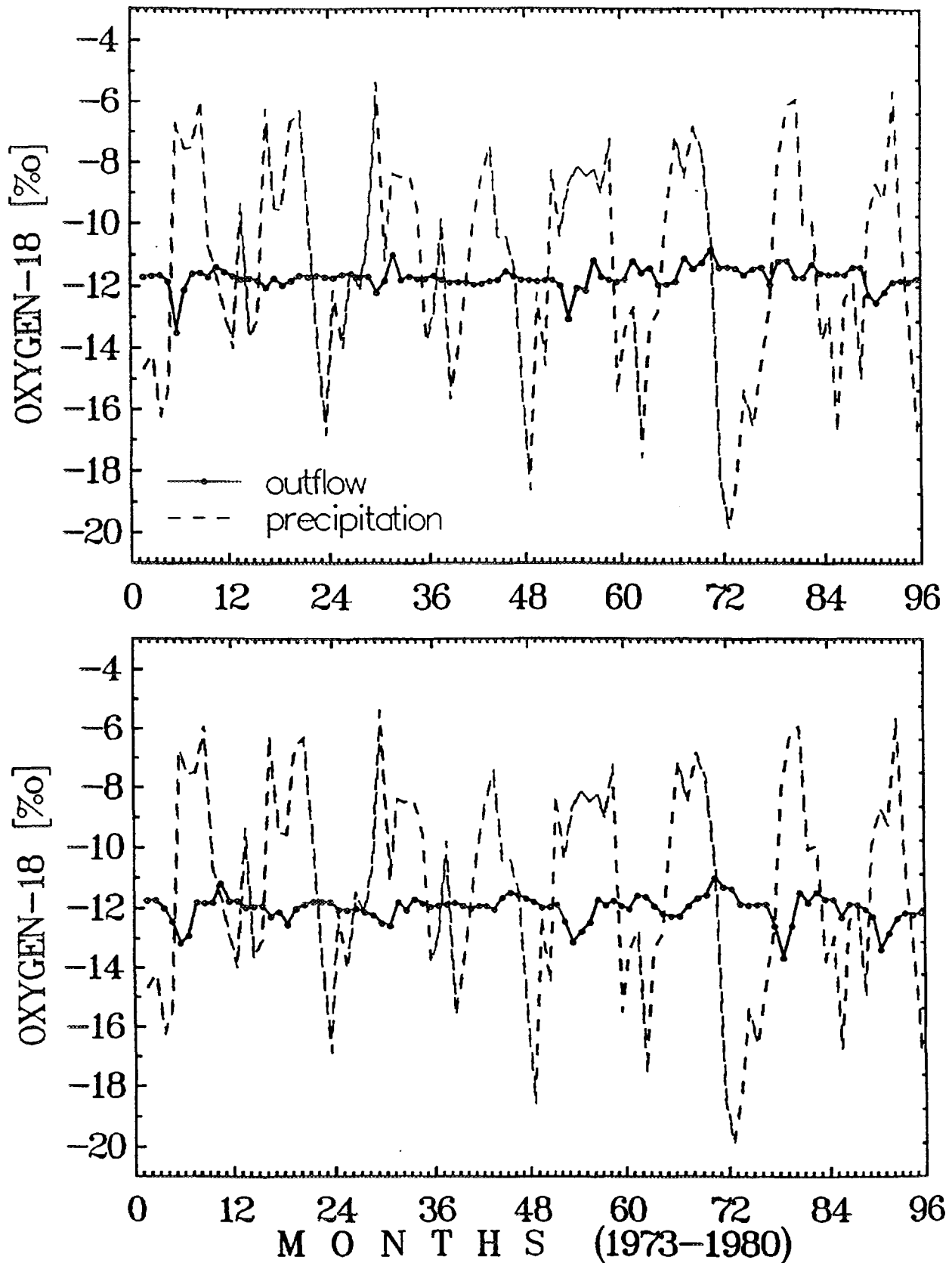


Fig. 22. Schneeealpe massif  $^{18}\text{O}$  output functions Wasseralquelle (upper) and Siebenquelle (lower) observed for high flows. Piston flow model (PFM) with  $t_t = 2$  months for both springs (only positions of maximal and minimal concentrations were fitted [64]).

(b) *An alpine karst massif, Schneealpe, Austria*

Changes in tritium and  $^{18}\text{O}$  contents were measured in water outflows from a karstic massif of  $90\text{ km}^2$  [64]. The conceptual model for tracer flow is given in Fig. 16. It was assumed that for base flow there is no flow in drainage channels. Then, tritium sampled in springs represented flow through the fissured porous aquifer. On the other hand, during high flow rates, the seasonal variations in  $^{18}\text{O}$  were assumed to represent the fast flow through channels. By fitting DM to the tritium data and PFM to the  $^{18}\text{O}$  data it was possible to find mean transit times for both sub-systems. Next, knowing the mean discharges for both flow components it was possible to estimate the water volumes of both subsystems.

Another complex karstic system which was identified by combination of artificial and environmental tracer methods was described in [65].

## REFERENCES

- [1] Eriksson, E., The possible use of tritium for estimating groundwater storage, *Tellus* **10** (1958) 472-478.
- [2] DAVIS, G.H., DINCER, T., FLORKOWSKI, T., PAYNE, B.R., GATTINGER, T., "Seasonal variations in the tritium content of groundwaters of the Vienna basin", *Isotopes in Hydrology*, IAEA, Vienna (1967) 451-473.
- [3] MAŁOSZEWSKI, P., ZUBER, A., Determining the turnover time of groundwater systems with the aid of environmental tracers, I. Models and their applicability, *J. Hydrol.* **57** (1982) 207-231.
- [4] PLUMMER, L.N., MICHEL, R.L., THURMAN, E.M., GLYNN, P.D., "Environmental tracers for age dating young ground water", *Regional Ground-Water Quality* (ALLEY, W.M., Ed.), Van Nostrand Reinhold, New York (1993) 255-294.
- [5] Nuclear Energy Agency (NEA), *The International Hydrocoin Project, Level 2: Model Validation*, Paris (1990).
- [6] ZUBER, A., "Mathematical models for the interpretation of environmental radioisotopes in groundwater systems", *Handbook of Environmental Isotope Geochemistry*, Vol. 2, Part B (FRITZ, P., FONTES, J.Ch., Eds.), Elsevier, Amsterdam (1986) 1-59.
- [7] MAŁOSZEWSKI, P., ZUBER, A., On the calibration and validation of mathematical models for the interpretation of tracer experiments in groundwater, *Adv. Water Resour.* **15** (1992) 47-62.
- [8] MAŁOSZEWSKI, P., ZUBER, A., Principles and practice of calibration and validation of mathematical models for the interpretation of environmental tracer data in aquifers, *Adv. Water Resour.* **16** (1993) 173-190.
- [9] ZUBER, A., "On calibration and validation of mathematical models for the interpretation of environmental tracer data in aquifers" IAEA-TECDOC, IAEA, Vienna (in press).
- [10] KONIKOV, L.F., BREDEHOEFT, J.D., Ground-water models cannot be validated, *Adv. Water Resour.* **15** 1 (1992) 75-83.
- [11] ORESKES, N., SHRADER-FRECHETTE, K., BELITZ, K., Verification, validation, and confirmation of numerical models in the earth sciences, *Science* **263** (1994) 641-646.
- [12] MAŁOSZEWSKI, P., ZUBER, A., Tracer experiments in fractured rocks: Matrix diffusion and the validity of models, *Water Resour. Res.*, **29** 8 (1993) 2723-2735.
- [13] ZUBER, A., MOTYKA, J., Matrix porosity as the most important parameter of fissured rocks for solute transport at large scales, *J. Hydrol.* **158** (1994) 19-46.
- [14] SNYDER, W.M., STALL, J.B., Men models, methods and machines in hydrologic analysis, *J. Hydraul. Div., ASCE*, **91** (1965) 85-99.
- [15] LEVENSPIEL, O., TURNER, J.C.R., The interpretation of residence time experiments. *Chem. Eng. Sci.* **25** (1970) 1605-1609.

- [16] GARDNER, R.P., FELDER, R.M., DUNN, T.S., Tracer concentration responses and moments for measurements of laminar flow in circular tubes, *Int. J. Appl. Radiat. Isot.* **24** (1973) 253-270.
- [17] BRIGHAM, W.E., Mixing equations in short laboratory cores, *Soc. Pet. Eng. J.* **14** (1974) 91-99.
- [18] KREFT, A., ZUBER, A., On the physical meaning of the dispersion equation and its solutions for different initial and boundary conditions, *Chem. Eng. Sci.* **33** (1978) 1471-1480.
- [19] ZUBER, A., "Review of existing mathematical models for interpretation of tracer data in hydrology", *Mathematical Models for Interpretation of Tracer Data in Groundwater Hydrology*, IAEA-TECDOC-381, IAEA, Vienna (1985) 69-116.
- [20] LENDA, A., ZUBER, A., "Tracer dispersion in groundwater experiments", *Isotope Hydrology 1970*, IAEA, Vienna, 619-641.
- [21] ANDERSEN, L.J., SEVEL, T., "Six years' environmental tritium profiles in the unsaturated and saturated zones", *Isotope Techniques in Groundwater Hydrology 1974*, Vol. I, IAEA, Vienna (1974) 3-20.
- [22] PRZEWŁOCKI, K., Hydrologic interpretation of the environmental isotope data in the Eastern Styrian Basin, *Steir. Beitr. Hydrol.* **27** (1975) 85-133.
- [23] IAEA, Tech. Rep. Ser., 96, 117, 129, 147, 129, 147, 165, 192, 206, 226, 264, 311, 331 (yearly means up to 1987 are given) IAEA, Vienna (newer data are available on diskettes only).
- [24] GRABCZAK, J., MAŁOSZEWSKI, P., RÓŻAŃSKI, K., ZUBER, A., Estimation of the tritium input function with the aid of stable isotopes, *Catena* **11** (1984) 105-114.
- [25] TOLSTIKHIN, I.N., KAMENSKY, I.L., Determination of groundwater ages by the T-<sup>3</sup>He method, *Geochemistry International* **6** (1969) 810-811.
- [26] TORGERSEN, T., CLARKE, W.B., JENKINS, W.J., "The tritium/helium-3 method in hydrology", *Isotope Hydrology 1978*, IAEA, Vienna, 917-930.
- [27] SCHLOSSER, P., STUTE, M., DORR, H., SONNTAG, C., MUNNICH, K.O., Tritium/<sup>3</sup>He dating of shallow groundwater, *Earth and Planetary Science Letters* **89** (1988) 353-362.
- [28] SCHLOSSER, P., STUTE, M., SONNTAG, C., MUNNICH, K.O., Tritiogenic <sup>3</sup>He in shallow groundwater, *Earth and Planetary Science Letters* **94** (1989) 245-256.
- [29] SOLOMON, D.K., SUDICKY, E.A., Tritium and helium-3 isotope ratios for direct estimation of spatial variations in groundwater recharge. *Water Resour. Res.* **27** 9 (1991) 2309-2319.
- [30] SOLOMON, D.K., POREDA, R.J., SCHIFF, S.L., CHERRY, J.A., Tritium and helium-3 as groundwater age tracers in the Borden aquifer, *Water Resour. Res.* **28** 3 741-755.
- [31] MAŁOSZEWSKI, P., ZUBER, A., The theoretical possibilities of the <sup>3</sup>H-<sup>3</sup>He method in investigations of groundwater systems, *Catena* **10** (1983) 189-198.
- [32] GRABCZAK, J., ZUBER, A., MAŁOSZEWSKI, P., RÓŻAŃSKI, K., WEISS, W., ŚLIWKA, I., New mathematical models for the interpretation of environmental tracers in groundwaters and the combined use of tritium, C-14, Kr-85, He-3 and freon-11 methods, *Beitr. Geol. Schweiz - Hydrologie*, **28** (1982) 395-405.
- [33] RÓŻAŃSKI, K., Krypton-85 in the atmosphere 1950-1977: a data review. *Environ. Int.* **2** (1979) 139-143.
- [34] RÓŻAŃSKI, K., FLORKOWSKI, T., "Radioactive noble gases in the terrestrial environment" *Handbook of Environmental Isotope Geochemistry*, Vol. 2, Part B (FRITZ, P., FONTES, J.Ch., Eds.), Elsevier, Amsterdam (1986) 481-506.
- [35] WEISS, W., SARTORIUS, H., STOCKBURGER, H., "Global distribution of atmospheric Kr-85: A database for the verification of transport and mixing models", *Isotopes of Noble Gases as Tracers in Environmental Studies*, IAEA (1992) 29-63.

- [36] RÓŻANSKI, K., FLORKOWSKI, T., "Krypton-85 dating of groundwater", *Isotope Hydrology 1978*, Vol. II, IAEA, Vienna (1979) 949-961.
- [37] SMETHIE, W.M., Jr., SOLOMON, D.K., SCHIFF, S.L., MATHIEU, G.G., Tracing groundwater flow in the Bordon aquifer using krypton-85, *J. Hydrol.* **130** (1992) 279-297.
- [38] FONTES, J.Ch., GARNIER, J.M., Determination of the initial  $^{14}\text{C}$  activity of the total dissolved carbon: a review of the existing models and a new approach, *Water Resour. Res.* **15** (1979) 369-413.
- [39] FONTES, J.Ch., "Chemical and isotopic constraints on  $^{14}\text{C}$  dating of groundwater", *Radiocarbon After Four Decades* (TAYLOR, R.A., LONG A., KRA, R.S., Eds.) Springer-Verlag, New York (1992) 242-261.
- [40] BERGMAN, H., SACKL, B., MAŁOSZEWSKI, P., STICHLER, W., "Hydrological investigations in a small catchment area using isotope data series", *5th International Symposium on Underground Water Tracing*, Institute of Geology and Mineral Exploration (IGME), Athens, 1986.
- [41] MAŁOSZEWSKI, P., RAURET, W., TRIMBORN, P., HERRMANN, A., RAU, R., Isotope hydrological study of mean transit times in an alpine basin. *J. Hydrol.* **140** (1992) 343-360.
- [42] BUSENBERG, E., PLUMMER, L.N., Use of chlorofluorocarbons ( $\text{CCl}_3\text{F}$  and  $\text{CCl}_2\text{F}_2$ ) as hydrologic tracers and age-dating tools: The alluvium and terrace system of central Oklahoma, *Water Resour. Res.* **28** 9 (1992) 2257-2283.
- [43] REILLY, T.E., PLUMMER L.N., PHILLIPS, P.J., BUSENBERG, E., The use of simulation and multiple environmental tracers to quantify groundwater flow in a shallow aquifer. *Water Resour. Res.* **30** 2 (1994) 421-433.
- [44] MAISS, M., LEVIN, I., global increase of  $\text{SF}_6$  observed in the atmosphere, *Geophys. Res. Lett.* **21** 7 (1994) 569-572.
- [45] ZUBER, A., On the interpretation of tracer data in variable flow systems, *J. Hydrol.* **86** (1986) 45-57.
- [46] ZUBER, A., MAŁOSZEWSKI, P., STICHLER, W., HERRMANN, A., "Tracer relations in variable flow" *5th International Symposium on Underground Water Tracing*, IGME (Institute of Geology and Mineral Exploration), Athens (1986) 355-360.
- [47] MAŁOSZEWSKI, P., (in preparation).
- [48] NERETNIEKS, I., Age dating of groundwater in fissured rocks: influence of water volume in micropores. *Water Resour. Res.* **17** (1981) 421-422.
- [49] MAŁOSZEWSKI, P., ZUBER, A., On the theory of tracer experiments in fissured rocks with a porous matrix, *J. Hydrol.* **79** (1985) 333-358.
- [50] MAŁOSZEWSKI, P., ZUBER, A., Influence of matrix diffusion and exchange reactions on radiocarbon ages in fissured carbonate aquifers, *Water Resour. Res.* **27** (1991) 1937-1945.
- [51] MAŁOSZEWSKI, P., *Mathematical Modelling of Tracer Experiments in Fissured Aquifers*, *Freiburger Schriften zur Hydrologie*, Band 2, Universität Freiburg, Freiburg (1994).
- [52] ZUBER, A., KLECZKOWSKI, A.S., MYSZKA, J., WITCZAK, S., "Pumping rate and mineralization of water from an intake at the high terrace of Vistula, east of Cracow, as explained by isotopic investigations" (in Polish), *Aktualne problemy hydrogeologii*, AGH, Kraków (1985) 186-195.
- [53] MAŁOSZEWSKI, P., RAUERT, W., TRIMBORN, P., HERRMANN, A., RAU, R., Isotope hydrological study of mean transit times in an alpine basin (Wimbachtal, Germany), *J. Hydrol.* **140** (1992) 343-360.
- [54] STICHLER, W., MAŁOSZEWSKI, P., MOSER, H., Modelling of river water infiltration using oxygen-18 data, *J. Hydrol.* **83** (1986) 355-365.
- [55] HÖTZL, H., REICHERT, B., MAŁOSZEWSKI, P., MOSER, H., STICHLER, W., "Contaminant transport in bank filtration - Determining hydraulic parameters by means of artificial and natural labeling", *Contaminant Transport in Groundwater* (KOBUS, H.E., KINZELBACH, W, Eds), A.A. Balkema, Rotterdam (1989) 65-71.

- [56] MAŁOSZEWSKI, P., MOSER, H., STICHLER, W., BERTLEFF, B., HEDIN, K., "Modelling of groundwater pollution by river bank filtration using oxygen-18 data", *Groundwater Monitoring and Management*, IAHS Publ. no. 173 (1990) 153-161.
- [57] CIEŻKOWSKI, W., GRÖNING, M., LESNIAK, P.M., WEISE, S.M., ZUBER, A., Origin and age of thermal waters in Cieplice Spa, Sudeten, Poland, inferred from isotope and noble gas data. *J. Hydrol.* **140**: 89-117.
- [58] ZUBER, A., WEISE, S.M., OSENBRÜCK, K., GRABCZAK, J., CIEŻKOWSKI, W., Age and recharge area of thermal waters in Łądek Spa (Sudeten, Poland) deduced from environmental isotope and noble gas data. *J. Hydrol.* (in press).
- [59] DAVIS, G.H., LEE, K.CH., BRADLEY, E., PAYNE, B.R., Geohydrologic interpretations of a volcanic island from environmental isotopes. *Water Resour. Res.* **6** (1970) 99-109.
- [60] MAŁOSZEWSKI, P., RAUERT, W., STICHLER, W., HERRMANN, A., Application of flow models in alpine catchment area using tritium and deuterium data, *J. Hydrol.* **66** (1983) 319-330.
- [61] HERRMANN, A., KOLL, J., MAŁOSZEWSKI, P., RAUERT, W., STICHLER, W., Water balance studies in a small catchment area of paleozoic rock using environmental isotope tracer techniques" *Conjunctive Water Use*, IAHS Publ. no. 156 (1986) 111-124.
- [62] HERRMANN, A., KOLL, J., LEIBUNGUT, CH., MAŁOSZEWSKI, P., RAU, R., RAUERT, W., SCHÖNIGER, M., STICHLER, W., Wasserumsatz in einem kleinem Einzugsgebiet im paläozoischen Mittelgebirge (Lange Bramke, Oberharz). Eine hydrologische Systemanalyse mittels Umweltisotopen als Tracer, *Landschaftökologie u. Umweltforschung*, Heft 17 (1989) 1-186.
- [63] MOTYKA, J., WITCZAK, S., ZUBER, A., Migration of lignosulphonates in a karstic-fractured-porous aquifer - history and prognosis for a Zn-Pb mine, Pomorzany, southern Poland, *Environ. Geol.* (1994) (in press).
- [64] RANK, D., VÖLKL, G., MAŁOSZEWSKI, P., STICHLER, W., "Flow dynamics in an alpine karst massif studied by means of environmental isotopes", *Isotope Techniques in Water Resources Development 1991*, IAEA, Vienna (1992) 327-343.
- [65] MAŁOSZEWSKI, P., HARUM, T., BENISCHKE, R., "Mathematical modelling of tracer experiments in the karst of Lurbach system", *Transport Phenomena in Different Aquifers*, *Steirische Beiträge zur Hydrologie*, Band 43 (1992) 116-136.
- [66] MAŁOSZEWSKI, P., HARUM, T., ZOJER, H., "Modelling of environmental tracer data", *Transport Phenomena in Different Aquifers*, *Steirische Beiträge zur Hydrologie*, Band 43 (1992) 136-143.
- [67] TAYLOR, G., Dispersion of soluble matter in solvent flowing slowly through a tube, *Proc. R. Soc. London, Ser. A*, **219** (1953) 186-203.
- [68] SUDICKY, E.A., FRIND, E.O., Contaminant transport in fractured porous media: Analytical solutions for a system of parallel fractures, *Water Resour. Res.* **18** (1982) 1634-1642.

**APPENDIX A: Examples of tracer curves (system response functions) for different injection-detection modes**

A capillary with a laminar flow can be regarded as one of the simplest systems, though the transport of solute is quite complex. At a short distance the influence of molecular diffusion is negligible and one may assume that tracer particles do not move from one flow line to another, and, consequently the observed tracer distribution results only the parabolic distribution of flow velocity and from the injection-detection mode. For an instantaneous injection the following formulas are obtained [16, 19]:

$$C_{IRR}(t) = (M/2V)/(t/t_w) \quad (A.1)$$

$$C_{IRF}(t) = C_{IFR}(t) = (M/2V)/(t/t_w)^2 \quad (A.2)$$

$$C_{IFF}(t) = (M/2V)/(t/t_w)^3 \quad (A.3)$$

for  $t \geq 0.5t_w$

and  $C(t) = 0$  for  $t < 0$

where  $M$  is the injected mass,  $V$  is the volume of water in the capillary between the injection and detection cross-section and  $t_w$  is the mean transit

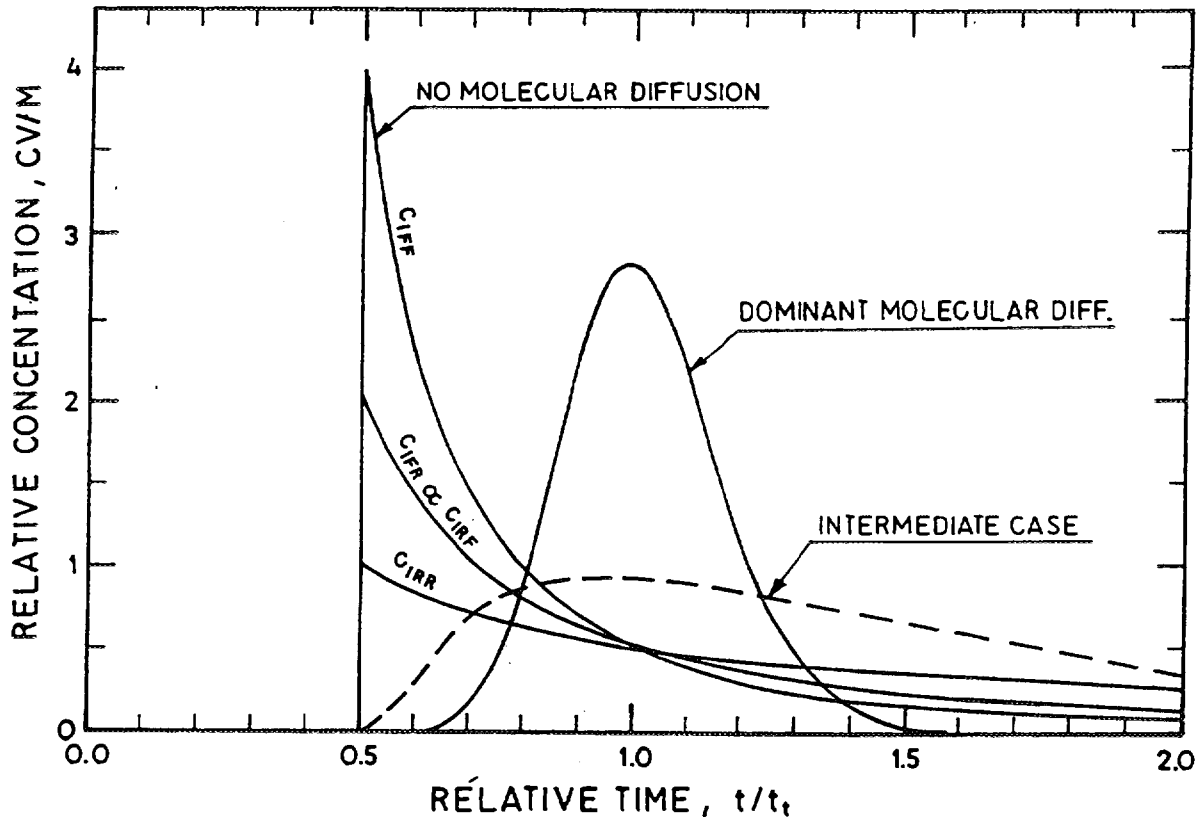


Fig. A.1. Normalized response functions for laminar flow in a capillary for negligible molecular diffusion (they depend on injection-detection mode), and typical examples of response functions in case of dominant molecular diffusion and under intermediate conditions [19].

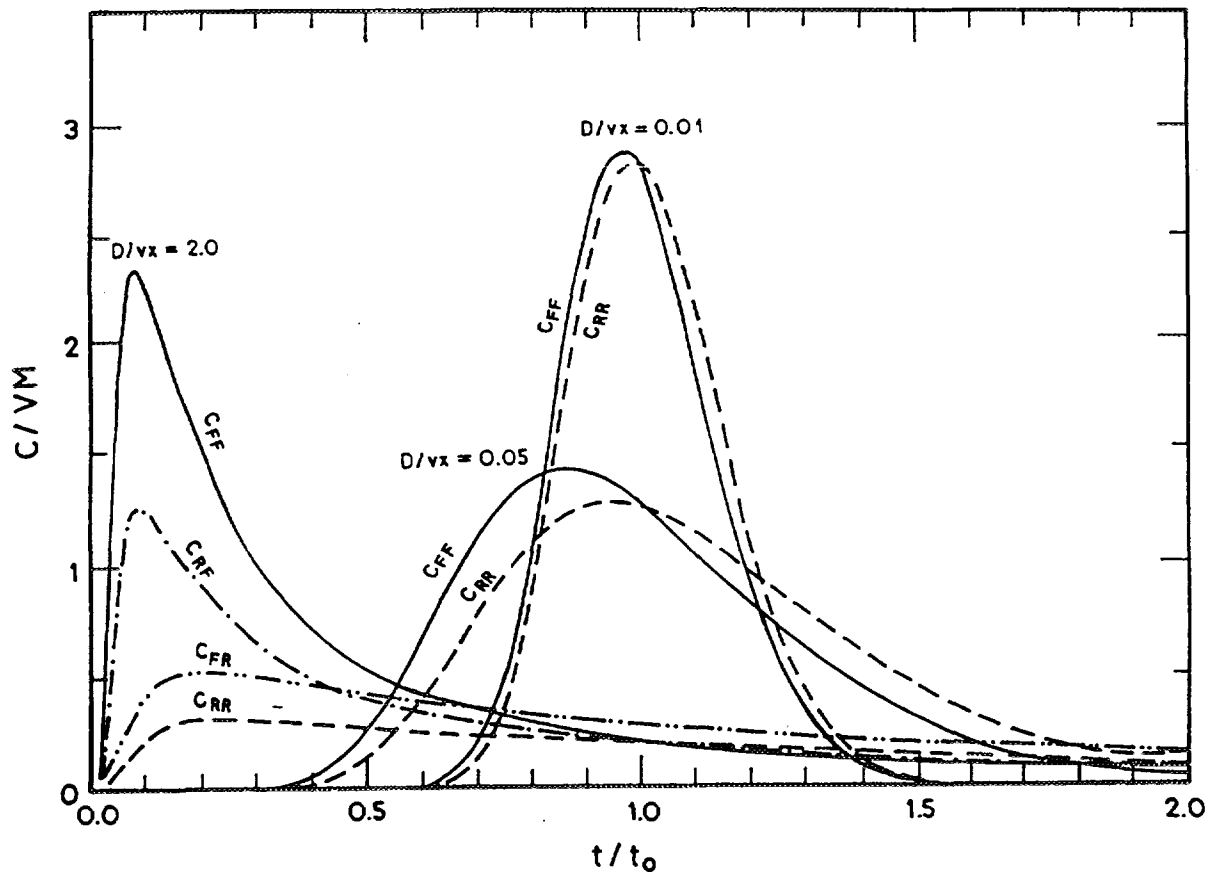


Fig. A.2. Examples of normalized response functions for different injection-detection modes in case of DM (dispersion model) [19].

time (exit age, turnover time) of water defined as  $t_w = V/Q$  ( $Q$  being the volumetric flow rate).

Relative tracer curves (which after dividing by  $t_w$  are equal to the system response functions) are given in Fig. A.1 as cases with no molecular diffusion. It is easy to check that only for Eq. A.3 the mean transit time of tracer (age of tracer) defined by Eq. 8 is equal to the mean transit time of water.

If a capillary is long enough, or/and the mean flow velocity is sufficiently low for the molecular diffusion to become a dominant process in the transverse mixing, the tracer is distributed around the mean transit time of water and the tracer curve is given by a solution to the dispersion equation [67] (an example shown in Fig. A.1 by the curve for dominant molecular diffusion).

For the intermediate cases, no theoretical formula is available. Then, the tracer curves are flat with a long tail (an example shown in Fig. A.1).

In conclusion, the behaviour of a tracer in a capillary, though dependent on the distribution of flow line velocities, does not represent the system in a unique way, because it also depends on the injection-detection mode as well as on the duration of an experiment and the coefficient of molecular diffusion.

Similarly, for systems which can be described by solutions to the dispersion equation, four injection-detection modes exist [19]. In Fig. A.2 examples of tracer curves for three chosen values of the dispersion parameter ( $D/vx = Pe^{-1}$ ) are shown. It is clear that for low values of the dispersion parameter (high Peclet numbers), the influence of the injection-detection mode becomes negligible.



**APPENDIX B: An example of differences observed in fissured rocks between the water age ( $t_w$ ), conservative tracer age ( $t_t$ ), and radioisotope age ( $t_a$ )**

Differences between the mean time travel times (ages) of mobile water ( $t_w$ ), conservative solute ( $t_t$ ), and decaying tracer ( $t_a$ ), or the mean velocities of mobile water ( $v_w$ ), conservative solute ( $v_t$ ), and decaying tracer ( $v_a$ ), can be easily demonstrated in a number of ways. An exact analytical solution to the transport equation in the fissures coupled with the diffusion equation in the matrix, for a system of parallel fissures of equal spacing and apertures, is chosen after [13] to serve the purpose. That solution yields the tritium distributions along flow in fissures in the case of a constant input as shown in Fig. B.1 (adapted from Figs. 2 and 4 in [68]).

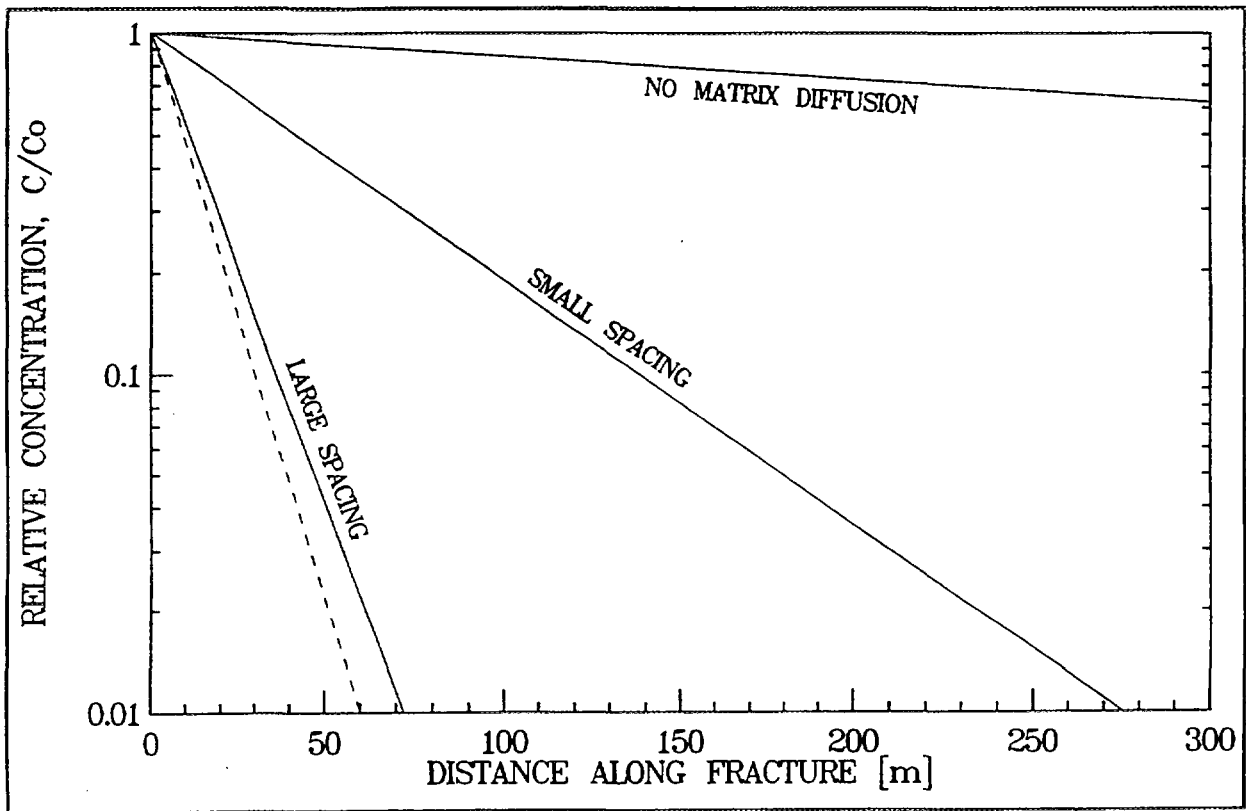


Fig. B.1. An example of the dependence of tracer age on matrix diffusion and the decay of tracer in the matrix (adapted from [13], original calculations after [67]). Case of no matrix diffusion shows the distribution of tritium in fissures when  $n_p = 0$  (other parameters given in text). Case of small spacing shows the distribution of tritium for fissure spacing of 0.1 m and matrix porosity of 0.01. This distribution is in a good approximation related to the case of no diffusion by Eq. 31. Case of large spacing (heavy line) shows the distribution of tritium for spacing of 0.5 m (other parameters as above). Dashed line shows the distribution which would be observed if there were no decay in the matrix (related to the case of no diffusion by Eq. 31 which is now less exact but still yields much better results than the assumption of no diffusion).

A matrix porosity of 0.01, and a fissure aperture of 100  $\mu\text{m}$  were assumed. The fissure spacing was 0.5 m (large spacing) and 0.1 m (small spacing). The boundary conditions were chosen in such a way that the flow velocity ( $v_w$ ) in fissures was in both cases equal to 0.1 m/d.

The fissure porosities are:  $0.0001\text{m}/0.5\text{m} = 0.0002$  and  $0.0001\text{m}/0.1\text{m} = 0.001$ , for large and small spacings, respectively. For these porosities, the retardation factors ( $R_p$ ) calculated from Eq. 31 are:  $(0.01 + 0.0002)/0.001 = 51$  and  $(0.01 + 0.001)/0.001 = 11$ , respectively.

For a steady state, the decaying tracer velocity ( $v_a$ ) can be calculated for any distance along the fissures. The distances at which the concentration is equal to 0.01 of the initial concentration are chosen here. For large and small fissure spacings these distances are: 72 m and 275 m, respectively (see Fig. B.1). In both cases, the decaying tracer age calculated from Eq. 19 is 82.4 years. The different values of velocities (in  $\text{m day}^{-1}$ ) are summarized as follows:

Velocity:	$v_w$	$v_t = x/t_t = v_w/R_p$	$v_a = x/t_a$
Large spacing:	0.1	0.00196	0.00239
Small spacing:	0.1	0.0091	0.0091

These results confirm the well-known fact of lower solute velocity in comparison with the flow (mobile water) velocity in fissures. They also show that, for large spacing, the decaying tracer velocity can be larger than the conservative tracer velocity, which is, unfortunately, not well known. In other words, the radioisotope ages defined by Eq. 19 can be lower than the conservative tracer ages in cases of sparsely fissured rocks. However, the differences between the conservative and decaying solute velocities and ages are either negligible or much lower than the differences between the solute and flow velocities. In densely fissured rocks, the differences between decaying and conservative tracer ages are negligible, particularly for large half-life times as in the case of radiocarbon [50].

The differences between exact Darcy's velocities and those estimated from the approximate form of Eq. 32 are also worth considering. For large spacing, the exact value is  $n_f v_w = 0.0002 \times 0.1 = 2 \times 10^{-5} \text{ m day}^{-1}$ , and the approximate one is  $n_p v_t = 0.01 \times 0.00196 = 1.96 \times 10^{-5} \text{ m/d}$ . For small spacing, these velocities are:  $0.1 \times 0.001 = 1 \times 10^{-4} \text{ m/d}$ , and  $0.01 \times 0.0091 = 0.91 \times 10^{-4} \text{ m day}^{-1}$ , respectively. It is obvious that even for as low  $n_p/n_f$  value as above (i.e.  $n_p/n_f = 10$ ), the approximate forms of Eqs 32 and 33 are sufficiently exact. Typical porosity ratios are higher, as shown in [13].